Master de Sciences et Technologies de l'UPMC
Mention Sciences de l'Ingénieur
Orientation Mécanique des Fluides : Fondements et Applications.

2009-2010

Propagation of Pulsated Waves in Viscoelastic Tubes: Application in Arterial Flows.

Audrey **G**ineau

Responsable: **P**ierre-**Y**ves **L**agrée – DR CNRS

Responsable :
P.Y. Lagrée
IJLRA- Université Pierre et Marie-Curie
4 Place Jussieu, 75252 Paris.
pierre-yves.lagree@upmc.fr

Abstract

We formulate a simple one-dimensional model for steady and pulsated flows in straight and viscoelastic tube. With a numerical simulation, we paid attention to the contributions of wall non-linear an viscous parameters presents in this model. We validate the theoretical analysis thanks to the simulation of the flows with the software COMSOL 3.4. Experimental measurements has been carried out for the same configuration of flows. Taking in account the different observed effects, we find a good agreement between experimental and numerical results, and we can confirm the predominant behaviour of the wall viscoelasticity. We introduce a biomechanical issue with the simulation of the pulsated flow in a viscoelastic tube that represents an aneurysm.

Nous présentons un modèle intégral simple mono dimensionnel en vue d'application pour les écoulements biomécaniques dans les artères. En pratique nous comparerons à une expérience d'écoulement dans un tube droit viscoélatique. Nous discutons la contribution des termes de viscosité fluide, de viscoélasticité et de non linéarité de fluide et de paroi. Nous comparons numériquement cette approche 1D à la résolution "complète" en axi-symétrique de l'intéraction fluide structure résolue avec le code commercial COMSOL. Ayant tenu compte de ces phénomènes principaux, nous observons un bon accord entre l'expérience et la simulation. Notamment, la viscoélasticité du tuyau a un rôle prédominant. En perspective, nous présentons un premier calcul dans une configuration pathologique d'une artère: l'anévrisme.

Thanks

First I thank **M. Pierre-Yves Lagrée** for receiving me during three months in the IJLRA. His incredible availability, as his advices, allowed me to work in the best conditions. With kindness ,he communicated all his interest and enthusiasm for working. Let him know I have a great deal of respect for him.

I thank also everyone I have spent time with, for their good mood all this internship long: Hubert, Jalil, Julie...
And I thank particularly Masashi Saito for his amazing kindness and, for always encouraging and helping me when hurdles come.

I thank M. Fullana for let me know this subject, for this availability and his help. I also wink him for receiving my whimpering with humour.

And finally, I thank every members of IJLRA like ,Elsa Vennat, Philippe Ressot, T. Ait Ali and also M. Patrick Flaud, who have helped and shared their precious knowledges.

1 Introduction

Studying cardiovascular and ventilatory fluid mechanics is fundamental to understand the progression and the origins of diseases. Alarming arterial diseases, like aneurysm or atherosclerosis, urge Biomechanics to be able to quantify the stresses into vascular tubes and prevent its wall damages.
Because of pulsated flows, non-linear and non-homogeneous behaviours of blood and arterial wall, the fluid mechanics of these systems is very complex.

We are interested in the pulsated flow in an artery with an aneurysm. We attempt to get closer of this complexity by only consider the viscoelastic and non-linear behaviour of cylindrical tubes. We note that viscoelasticity is also a property of Non-Newtonian fluids like blood (Fung, Horsten et *al.*).

An other challenge is making numerical simulations of these vascular flows using the full 3D formulation. A one-dimensional model including viscosity and non-linearities is an interesting alternative to avoid difficulty of 3D or 2D computations (P.-Y. Lagrée, Pindera et *al.*, J.M. Fullana et *al.*, Stergiopulos et *al.*, Van de Vosse et *al.*, Pedley, Zagzoule et *al.*).

The aim of this study is checking the validity of the one-dimensional model firstly by making a comparison with a code, COMSOL Multiphysics 3.4, computing with the 3D formulation of the Navier-Stokes equations. Here, only 2D and axisymmetrical computations will be done. The validity is also checked by making comparisons with measurements of a pulse propagation in viscoelastic tubes. This experiment has been carried out by M. Saito, a Ph.D. Student of Doshisha University Kyoto Japan, and his Professor M. Matsukawa.
The experiment shows that we can define a set of small parameters. This will guide us to model the flow.

First, the formulation of dimensionless equations for a steady and pulsated flow in a rigid tube allows to introduce simple velocity profiles. Thanks to these velocity profiles we can write the final one-dimensional problem of a pulsated flow in a flexible tube.
But first, we use small parameters that appear in the flow configuration. For example pulse waves length widely dominates the tube's radius. Also the variation of the radius is very small compared to the radius. And more, the velocity of the flow is very small compared to the wave velocity.
The introduction of a pressure law including viscoelastic and non-linear properties of the tube wall allows to close the latest formulation. From there, equations are written with enough terms to describe the physics of the flow: we do have a minimal set of partial differential equations.
Then the influence of the solid viscosity and non-linearity on a wave propagation is highlighted.
As we know all different parameters' effects on a pressure pulse propagation, we can then validate the one-dimensional model, and quantify the both fluid and solid viscous and non-linear effects of the M. Saito's experiment.
As an opening on a one-dimensional simulation of arterial diseases, it will be finally presented results from COMSOL 3.4 simulation of the propagation of a pressure pulse in a "viscoelastic aneurysm".

2 Steady and Pulsated Flow in a Straight and Rigid Tube

Here, we introduce a theoretical analysis applied to rigid tubes in order to find simple velocity profiles that will be useful for elastic tube. These profiles give a good approximation of those that can be find in flexible tubes (J.M. Fullana et *al.*, P.-Y. Lagrée, Van de Vosse et *al.*).

2.1 Basic Equations

To study a incompressible Newtonian flow where the volumic forces are neglected, let us consider the Navier-Stokes equations. These are the mass conservation equation (or the continuity equation) and the momentum equation which reads:

$$Div\mathbf{V} = 0,$$

$$\frac{\partial \mathbf{V}}{\partial t} + \mathbf{V} \cdot \overline{\overline{Grad}}\mathbf{V} = \frac{1}{\rho}\, \overline{Grad}\, p + \nu\, \Delta \mathbf{V}.$$

Let us consider a steady and pulsated flow in a straight and rigid tube of radius R is and frequency ω. As a first approximation, we consider an uni-axial flow. So, in the cylindrical coordinate system with $\mathbf{V} = u\vec{ex} + v\vec{er}$, the latest Navier-Stokes equations are given by:

$$\frac{\partial u}{\partial x} + \frac{1}{r}\frac{\partial (rv)}{\partial r} = 0, \tag{1}$$

$$\frac{\partial u}{\partial t} + u\frac{\partial u}{\partial x} + v\frac{\partial u}{\partial r} = -\frac{1}{\rho}\frac{\partial p}{\partial x} + \nu\,(\frac{1}{r}\frac{\partial}{\partial r}(r\frac{\partial u}{\partial r}) + \frac{\partial^2 u}{\partial x^2}), \tag{2}$$

$$\frac{\partial v}{\partial t} + u\frac{\partial v}{\partial x} + v\frac{\partial v}{\partial r} = -\frac{1}{\rho}\frac{\partial p}{\partial r} + \nu\,(\frac{\partial}{\partial r}(\frac{1}{r}\frac{\partial (rv)}{\partial r}) + \frac{\partial^2 r}{\partial x^2}). \tag{3}$$

Let us first make the variables dimensionless:

$$x = L_e\bar{x} \quad r = R\bar{r} \quad t = \frac{\bar{t}}{\omega} \quad p = p_o + \delta p \cdot \bar{p} \quad u = U_o\bar{u} \quad v = V_o\bar{v}\ ,$$

and then examine the mass conservation equation:

$$\frac{U_o}{L_e}\frac{\partial \bar{u}}{\partial \bar{x}} + \frac{V_o}{R}\frac{1}{\bar{r}}\frac{\partial (\bar{r}\bar{v})}{\partial \bar{r}} = 0.$$

By a *reductio ad absurdum*, we conclude easily that the scale of the radius component is negligible in the motion equations.

$\diamond$ Let's imagine that $\dfrac{U_o}{L_e} \ll \dfrac{V_o}{R}$.

So the second term is dominant and a first approximation gives $\dfrac{\partial (\bar{r}\bar{v})}{\partial \bar{r}} = 0$. This equation can be integrated, and has $\bar{v} = Constant(\bar{x})/\bar{r}$ as a solution; which is

physically not possible near the axis.

$\diamond$ And if $\frac{U_o}{L_e} \gg \frac{V_o}{R}$, the second term is negligible and a first approximation gives $\frac{\partial \bar{u}}{\partial \bar{x}} = 0$. This would mean that $\bar{u} = \bar{u}(\bar{r})$, and so, the flow would not change with the axial direction. This case is also unacceptable.

So The only one possibility is taking $\frac{U_o}{L_e} \sim \frac{V_o}{R}$, and setting $V_o = \varepsilon U_o$ where $\varepsilon = \frac{R}{L_e}$. Taking this parameter into account, the motion equations read:

$$\frac{\partial \bar{u}}{\partial \bar{x}} + \frac{1}{\bar{r}} \frac{\partial (\bar{r}\bar{v})}{\partial \bar{r}} = 0, \tag{4}$$

$$\frac{L_e \omega}{U_o} \frac{\partial \bar{u}}{\partial \bar{t}} + \bar{u} \frac{\partial \bar{u}}{\partial \bar{x}} + \bar{v} \frac{\partial \bar{u}}{\partial \bar{r}} = -\frac{\delta p}{\rho U_o^2} \frac{\partial \bar{p}}{\partial \bar{x}} + \frac{1}{\varepsilon^2} \frac{\nu}{U_o L_e} \left(\frac{1}{\bar{r}} \frac{\partial}{\partial \bar{r}} (\bar{r} \frac{\partial \bar{u}}{\partial \bar{r}}) + \varepsilon^2 \frac{\partial^2 \bar{u}}{\partial \bar{x}^2}\right), \tag{5}$$

$$\frac{L_e \omega}{U_o} \frac{\partial \bar{v}}{\partial \bar{t}} + \bar{u} \frac{\partial \bar{v}}{\partial \bar{x}} + \bar{v} \frac{\partial \bar{v}}{\partial \bar{r}} = -\frac{1}{\varepsilon^2} \frac{\delta p}{\rho U_o^2} \frac{\partial \bar{p}}{\partial \bar{r}} + \frac{1}{\varepsilon^2} \frac{\nu}{U_o L_e} \left(\frac{\partial}{\partial \bar{r}} (\frac{1}{\bar{r}} \frac{\partial (\bar{r}\bar{v})}{\partial \bar{r}}) + \varepsilon^2 \frac{\partial^2 \bar{v}}{\partial \bar{x}^2}\right) \tag{6}$$

Hypothesis allow to simply these Navier-Stokes equations thanks to a *phenomenological analysis (Monavon).*

As we undertake this study in order to an implementation to flows in vascular system, we will stay in the fully developed flow case. That means that the entrance effects are neglected and the flow will be studied from the region where the boundary layers meet each other (Figure 1). From here we assert that the entrance length is prevailing on the radius' scale:

$$L_e \gg R.$$

Indeed, we could show that $L_e \approx Re_R R$, where $Re_R = \frac{U_o R}{\mu}$

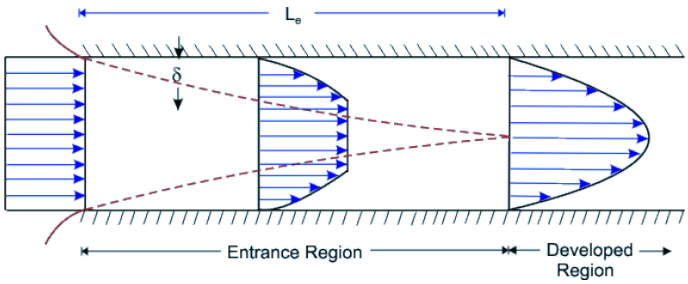

Figure 1: ***Fully developed flow***
Internet sources [1]

Regarding to the latest hypothesis, we have $\varepsilon \ll 1$. So it comes that $V_o \ll U_o$. And after keeping only the predominant terms, we're about to study:

$$\frac{\partial u}{\partial x} = 0, \tag{7}$$

$$\frac{\partial u}{\partial t} = -\frac{1}{\rho}\frac{\partial p}{\partial x} + \nu \, \frac{1}{r}\frac{\partial}{\partial r}(r\frac{\partial u}{\partial r}), \tag{8}$$

$$0 = -\frac{1}{\rho}\frac{\partial p}{\partial r}. \tag{9}$$

We will assume a harmonic pressure, and will search for harmonics solutions. Regarding to the equations (7) and (9), we have:

$$u = u(r,t) = u(r) \cdot e^{iwt} \quad p = p(x,t) = p(x) \cdot e^{iwt},$$

with:

$$p(x) = p_o + \delta p \cdot \bar{p}(\bar{x}) \quad u(r) = U_o \bar{u}(\bar{r}).$$

By dropping e^{iwt} in the momentum equation (8), we obtain this following dimensionless equation:

$$i \; \bar{u} = -\frac{\delta p}{\rho \omega U_o^2}\frac{\partial \bar{p}}{\partial \bar{x}} + \frac{\nu}{R\omega} \; \frac{1}{\bar{r}}\frac{\partial}{\partial \bar{r}}(\bar{r}\frac{\partial \bar{u}}{\partial \bar{r}}). \tag{10}$$

If we introduce the Womersley number α, and the Reynolds number Re defined by :

$$\alpha = R\sqrt{\frac{\omega}{\nu}}.$$

we finally obtain:

$$i \; \bar{u} = -\frac{\delta p}{\rho \omega U_o^2}\frac{\partial \bar{p}}{\partial \bar{x}} + \frac{1}{\alpha^2} \; \frac{1}{\bar{r}}\frac{\partial}{\partial \bar{r}}(\bar{r}\frac{\partial \bar{u}}{\partial \bar{r}}). \tag{11}$$

Nota Bene:

We note that $\alpha^2 = Sr \; Re$, where Sr and Re are the Strouhal and the Reynolds numbers:

$$Sr = \frac{\omega R}{U_o} \quad and \quad Re = \frac{U_o R}{\nu}.$$

2.2 A solution depending on the Womersley number

The coming study needs to be provided by simple velocity profiles. So let us find some, and confirm them thanks to the analytic solution (Pedley, Van de Vosse et *al.*).

2.2.1 Analytic solutions

The exact solution of the equation (10) is the sum of a particular solution and the solution of its homogeneous equation. From now, we drop the - over the variables, and we call $\Pi(\bar{x}) = \frac{\delta p}{\rho \omega U_o^2}\frac{\partial \bar{p}}{\partial \bar{x}}$ the pressure gradient term:

$$i \; u = -\Pi + \frac{1}{\alpha^2} \; \frac{1}{r}\frac{\partial}{\partial r}(r\frac{\partial u}{\partial r}).$$

$\diamond$ *A particular solution:*
A possible particular solution is :

$$u_p = i\Pi.$$

$\diamond$ *Solution of homogeneous equation:*
We search for the solution of

$$\frac{1}{\alpha^2}\,\frac{1}{r}\frac{\partial}{\partial r}(r\frac{\partial u}{\partial r}) - i\,u = 0.$$

which is an equation of the same form that the Bessel one, and whom the solutions are the Bessel functions.

Nota Bene:

The equation of Bessel:

$$\frac{\partial^2 f}{\partial x^2} + \frac{1}{x}\frac{\partial f}{\partial x} + (1 - \frac{n^2}{x^2})f = 0,$$

has solutions given by the Bessel functions of the first kind:

$$f(x) = J_n(x) = \sum_{k=0}^{\infty} \frac{(-1)^k}{k!(n+k)!}\left(\frac{x}{2}\right)^{2k+n}.$$

(Pedley, Womersley).

After developing the first derivative, we can rewrite the homogeneous equation as following:

$$\frac{\partial^2 u}{\partial(r\alpha i^{\frac{3}{2}})^2} + \frac{1}{r\alpha i^{\frac{3}{2}}}\frac{\partial u}{\partial(r\alpha i^{\frac{3}{2}})} + \; u = 0,$$

and then have for n = 0 :

$$u_h = A \cdot J_0(r\alpha i^{\frac{3}{2}}).$$

Using the boundary condition on the wall, $u(r=1) = (u_p + u_h)(r=1) = 0$, we determine the constant:

$$A = -\frac{i\Pi}{J_0(\alpha i^{\frac{3}{2}})}.$$

And finally,

$$\bar{u}(\bar{r}) = i\Pi(\bar{x})\left(1 - \frac{J_0(\bar{r}\alpha i^{\frac{3}{2}})}{J_0(\alpha i^{\frac{3}{2}})}\right). \tag{12}$$

Examples of profiles are plotted on Figure 2 for various values of α.

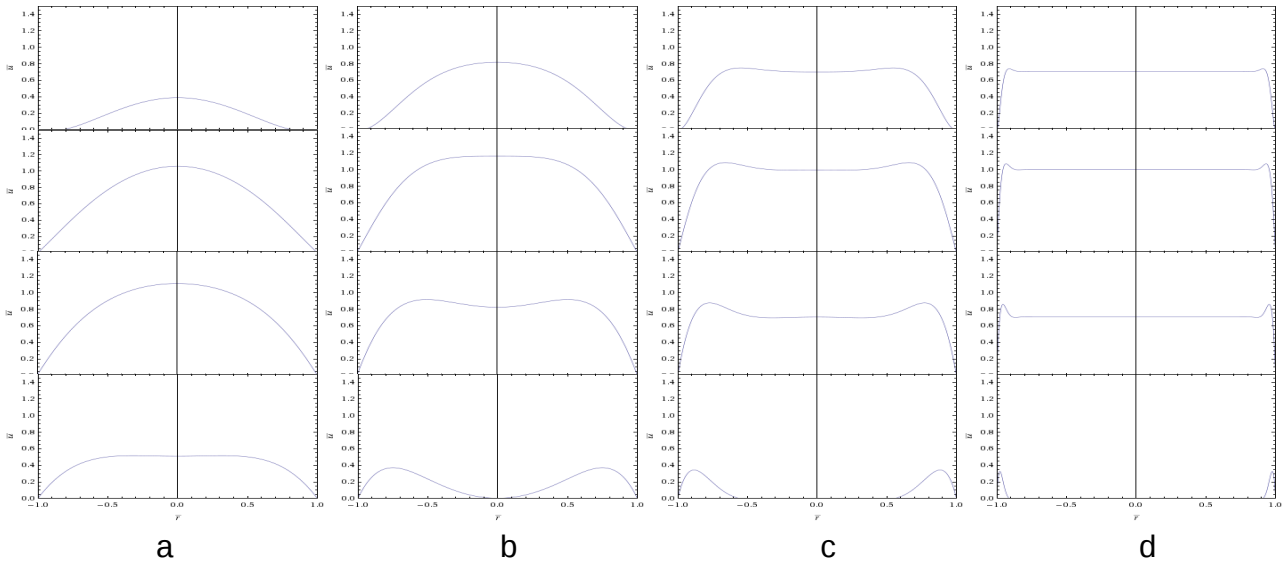

Figure 2: ***Various velocity profiles for*** $t = \pi/2$ ***to*** $3\pi/4$***; from left to right for*** $\alpha = 3\ 5\ 50,\ 100$**.** We do observe the Poiseuille effect for a small α, beside the velocity profile is flat for a large one.

2.2.2 Small Womersley number flow

In the case of $\alpha \to 0$, viscous forces prevail on inertial's ones, and inertial forces do not contribute so much the flow's behaviour. So a first approximation of the equation (10) gives:

$$0 = -\frac{\delta p}{\rho \omega U_o^2}\frac{\partial \bar{p}}{\partial \bar{x}} + \frac{1}{\alpha^2}\ \frac{1}{\bar{r}}\frac{\partial}{\partial \bar{r}}(\bar{r}\frac{\partial \bar{u}}{\partial \bar{r}}).$$

Nota Bene:
Physic proprieties of the flow need to be underline.
Pressure forces have to be considered as driver of the flow, since they're acting on the axial direction. But it appears that (not only in fluid dynamics) a driver needs to be balanced by one or several "brakes". "Brakes" could be friction or viscous forces.
Applying this theory to the dimensionless equation (10), the pressure's scale verifies:

$$\frac{\delta p}{\rho \omega U_o^2} = Sup\left\{1; \frac{1}{\alpha^2}\right\},$$

where $1 = Re(i)$.
And we do have the latest approximation in the case of low value of α .

Let's keep $\Pi(\bar{x}) = \dfrac{\delta p}{\rho \omega U_o^2}\dfrac{\partial \bar{p}}{\partial \bar{x}}$. After integrating $\dfrac{1}{\bar{r}}\dfrac{\partial}{\partial \bar{r}}(\bar{r}\dfrac{\partial \bar{u}}{\partial \bar{r}}) = \alpha^2\Pi(\bar{x})$, using no slip boundary layer $\bar{u}(\bar{r}=1) = 0$, and the axisymmetrical one $\dfrac{\partial \bar{u}}{\partial \bar{r}})_{\bar{r}=0} = 0$, we find:

$$\bar{u}(\bar{r}) = -\frac{\alpha^2}{4}\Pi(1-\bar{r}^2). \tag{13}$$

So, for a small Wormersley number, a Poiseuille profile is found as expected.

(Von de Vosse et *al.*)

2.2.3 Large Womersley number flow

In the case $\alpha \to \infty$, inertial forces prevail on viscous ones. But here, we cannot neglected a term of the flow equation like previously because viscous effects do exist near the wall.
Let us make this following change of variable $\bar{r} = 1 - \varepsilon\hat{r}$, where $\hat{r}$ represents the radial variation of the boundary layer, and ε a very small parameter. Let us take back the full dimensionless momentum equation (10)

$$i\ \bar{u} = -\Pi + \frac{1}{\alpha^2}\ \frac{1}{\bar{r}}\frac{\partial}{\partial\bar{r}}(\bar{r}\frac{\partial\bar{u}}{\partial\bar{r}}),$$

examine the last term, and hold a first order approximation. It finally yields:

$$i\ \bar{u} = -\Pi + \frac{1}{\alpha^2\varepsilon^2}\ \frac{\partial^2\bar{u}}{\partial\hat{r}^2}.$$

No simplification is possible as $\alpha \gg 1$ and $\varepsilon \ll 1$. So the good alternative, by reductio ad absurdum, is setting $\frac{1}{\alpha^2\varepsilon^2} \sim 1$, and the equation to solve becomes:

$$i\ \bar{u} = -\Pi + \ \frac{\partial^2\bar{u}}{\partial\hat{r}^2}.$$

$\diamond$ *A particular solution:*
A possible particular solution is :

$$u_p = i\Pi.$$

$\diamond$ *Solution of homogeneous equation:*
We search for the solution of

$$\frac{\partial^2\bar{u}}{\partial\hat{r}^2} = i\ \bar{u},$$

whom the solution is $\bar{u} = a \cdot e^{-p\hat{r}} + b \cdot e^{+p\hat{r}}$, where $p = i\frac{1}{2} = \frac{\sqrt{2}}{2}\ (1+i)$.

Using no-slip and uni-axial boundary conditions, we have :

$$\bar{u}(\hat{r}) = i\ \Pi(1 - e^{-p\hat{r}}).$$

And finally:

$$\bar{u}(\bar{r}) = i\ \Pi\ (1 - e^{-\alpha\frac{\sqrt{2}}{2}\ (1+i)\ (1-\bar{r})}). \tag{14}$$

Nota Bene:

We can observe with plots that the both solutions [13] and [14] are the limits of the analytical solution [12] when the Womersley number is small or large.

2.3 Conclusion.

We have computed the pulsated flow in a straight and rigis tube. These latest analytical solutions provide interesting simplifications for those in vascular systems (Von de Vosse et *al.*, P.-Y. Lagrée, J.M. Fullana, Zagzoule et *al.*, Pindera et *al.*, Stergiopulos et *al.*). We are now about to use them for flow in straight and flexible tubes.

3 Steady and Pulsated Flow in a Flexible Tube

Let us consider the flow in a circular elastic tube by using the results of the previous analysis.
In addition to introducing elastic materials effects on the flow, we are going to be interested in the rate of flow $Q = \int_S \mathbf{V} \cdot \mathbf{S}\, ds$ rather than the velocity. Indeed, in order to implement this study to a large variety of fluids, it's better to look after the rate of flow which does not reveal as much as fluid particles' velocity, the non-homogeneous properties of fluids.
Moreover, it is more interesting to work out rate of flow since characteristic of cardiovascular circulation are obtained experimentally by measuring it.

3.1 Basic Equations

Let $R = R_o + \Delta R$ be the radius of the flexible tube where ΔR is a small disturbance of the stable state R_o.

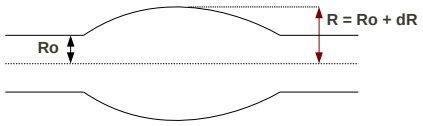

Figure 3: ***Deformation of elastic tube of initial radius Ro***

This disturbance does not allow to be in the case of fully developed flow. Then, we do not have any more as mass conservation equation $\frac{\partial u}{\partial x} = 0$.

Let us come back to the system of equations [(4), (5), (6)].

$$\frac{\partial \bar{u}}{\partial \bar{x}} + \frac{1}{\bar{r}}\frac{\partial(\bar{r}\bar{v})}{\partial \bar{r}} = 0,$$
$$\frac{L_e}{U_o\omega}\frac{\partial \bar{u}}{\partial \bar{t}} + \bar{u}\frac{\partial \bar{u}}{\partial \bar{x}} + \bar{v}\frac{\partial \bar{u}}{\partial \bar{r}} = -\frac{\delta p}{\rho U_o^2}\frac{\partial \bar{p}}{\partial \bar{x}} + \frac{1}{\varepsilon^2}\frac{\nu}{U_o L_e}\,(\frac{1}{\bar{r}}\frac{\partial}{\partial \bar{r}}(\bar{r}\frac{\partial \bar{u}}{\partial \bar{r}}) + \varepsilon^2\frac{\partial^2 \bar{u}}{\partial \bar{x}^2}),$$
$$\frac{L_e}{U_o\omega}\frac{\partial \bar{v}}{\partial \bar{t}} + \bar{u}\frac{\partial \bar{v}}{\partial \bar{x}} + \bar{v}\frac{\partial \bar{v}}{\partial \bar{r}} = -\frac{1}{\varepsilon^2}\frac{\delta p}{\rho U_o^2}\frac{\partial \bar{p}}{\partial \bar{r}} + \frac{1}{\varepsilon^2}\frac{\nu}{U_o L_e}\,(\frac{\partial}{\partial \bar{r}}(\frac{1}{\bar{r}}\frac{\partial(\bar{r}\bar{v})}{\partial \bar{r}}) + \varepsilon^2\frac{\partial^2 \bar{v}}{\partial \bar{x}^2}).$$

We still have $\varepsilon = \frac{R}{L_e} \ll 1$, and then $V_o \ll U_o$ regarding to the previous analysis of mass conservation equation. In the same way than the part 1.1, we keep only dominant terms:

$$\frac{\partial u}{\partial x} + \frac{1}{r}\frac{\partial(rv)}{\partial r} = 0, \tag{15}$$
$$\frac{\partial u}{\partial t} + u\frac{\partial u}{\partial x} + v\frac{\partial u}{\partial r} = -\frac{1}{\rho}\frac{\partial p}{\partial x} + \nu\,\frac{1}{r}\frac{\partial}{\partial r}(r\frac{\partial u}{\partial r}), \tag{16}$$
$$0 = -\frac{1}{\rho}\frac{\partial p}{\partial r}. \tag{17}$$

The equation [17] allows to assert that the pressure is constant across a tube section.

We are going to express this system of equations with the rate of flow, so let's make them under a conservative form:

$$\frac{\partial u}{\partial x} + \frac{1}{r}\frac{\partial (rv)}{\partial r} = 0, \tag{18}$$

$$\frac{\partial (ru)}{\partial t} + \frac{\partial (ruu)}{\partial x} + \frac{\partial (rvu)}{\partial r} = -\frac{r}{\rho}\frac{\partial p}{\partial x} + \nu \frac{1}{r}\frac{\partial}{\partial r}(r\frac{\partial u}{\partial r}). \tag{19}$$

$$\tag{20}$$

We integrate each term of these equations in order to bring out these following entities:

$$Q = \int_0^R 2\pi u r dr,$$

$$Q_u = \int_0^R 2\pi u^2 r dr.$$

We pay attention to the no slip conditions

$$u(r = R(x,t)) = 0 \quad and \quad v(r = R(x,t)) = \frac{\partial R}{\partial t} \quad ,$$

, and define the cross section of the tube as $S = \pi\ R^2$.

One of the convective term is cancelled because of this above condition. Indeed, we first use this derivative formulation:

$$\frac{\partial}{\partial x}\int_{\alpha(x)}^{\beta(x)} f(x,t)dt = \int_{\alpha(x)}^{\beta(x)} \frac{\partial f}{\partial x}(x,t)dt + \frac{\partial \alpha(x)}{\partial x} f(\alpha,t) - \frac{\partial \beta(x)}{\partial x} f(\beta,t)$$

Using this formulation for the last convective term yields:

$$2\pi \int_{r=0}^{r=R} \frac{\partial}{\partial r}(ruv)dr = \frac{\partial}{\partial r}\int_0^R 2\pi, ruv\ dr - \frac{\partial R}{\partial r}\ Ru(R)v(R) = 0$$

We finally obtain:

$$\frac{\partial Q}{\partial x} + \frac{\partial S}{\partial t} = 0, \tag{21}$$

$$\frac{\partial Q}{\partial t} + \frac{\partial Q_u}{\partial x} = -\frac{S}{\rho}\frac{\partial p}{\partial x} + 2\pi\nu R\left(\frac{\partial u}{\partial r}\right)_{r=R}. \tag{22}$$

The later system of equation shows two equations for five unknowns: Q, S, Q_u, p, and $\frac{\partial u}{\partial r}$. In the following part is going to be established a closure relation $Q_u = f(Q,S)$ and $\frac{\partial u}{\partial r} = f(Q,S)$, and next a pressure law $p = f(R)$.

3.2 A One-Dimensional Model depending on the Womersley number.

We have established simple velocity profiles depending on the value of the Womersley number. Let us use the results (12) and (13) of the part 2.2 in order to simplify the viscous and non-linear terms of the latest momentum equation.

3.2.1 Small Womersley number flow

For $\alpha \to 0$ the velocity profile is a Poiseuille's one (See part 2.2.1, equation (12)):

$$\bar{u}(\bar{r}) = -\frac{\alpha^2}{4}\Pi(1-\bar{r}^2).$$

So the rate of flow given by:

$$Q = \int_0^R 2\pi u r dr \; = \; \int_0^1 2\pi U_o R^2 \bar{u}\bar{r}d\bar{r},$$

yields

$$Q = (-\alpha^2\Pi)U_o \; \frac{\pi}{8}R^2. \tag{23}$$

$\diamond$ *Viscous term:*

$$2\pi\nu R\left(\frac{\partial u}{\partial r}\right)_{r=R} = 2\pi\nu R\frac{U_o}{R}\left(\frac{\partial \bar{u}}{\partial \bar{r}}\right)_{r=1} = -2\pi\nu R\frac{U_o}{R}\frac{(-\alpha^2\Pi)}{2} = -8\nu\frac{Q}{R^2}.$$

$\diamond$ *Non-linear term:*

$$Q_u = \int_0^R 2\pi u^2 r dr = \int_0^1 U_o^2 R^2 2\pi \bar{u}^2 \bar{r} d\bar{r} = \frac{\pi(-\alpha^2\Pi)^2 U_o^2 R^2}{48} = \frac{4}{3}\frac{Q^2}{\pi R^2}.$$

Here is the one-dimensional model for a low value of α:

$$\frac{\partial Q}{\partial x} + \frac{\partial S}{\partial t} \;\; = \;\; 0, \tag{24}$$

$$\frac{\partial Q}{\partial t} + \frac{4}{3}\frac{\partial}{\partial x}\frac{Q^2}{S} \;\; = \;\; -\frac{S}{\rho}\frac{\partial p}{\partial x} - 8\,\nu\frac{Q}{R^2}. \tag{25}$$

3.2.2 Large Womersley number flow

When $\alpha \to \infty$ the velocity profile is given by (See part 2.2.2, equation (13)):

$$\bar{u}(\bar{r}) = i\;\Pi\;(1 - e^{-\alpha\frac{\sqrt{2}}{2}\;(1+i)\;(1-\bar{r})}).$$

For a such Womersley number, we have observed cross a section, a quasi-constant velocity.Let Π be the velocity's amplitude. So we have as rate of flow :

$$Q = S\;U_o\Pi.$$

And so, the non-linear term is,

$$Q_u = S(U_o\Pi)^2 \; = \frac{Q^2}{S}$$

$\diamond$ *Viscous term:*

$$2\pi\nu R\left(\frac{\partial u}{\partial r}\right)_{r=R} = 2\pi\nu R\frac{U_o}{R}\left(\frac{\partial \bar{u}}{\partial \bar{r}}\right)_{r=1}, \text{ with } \left(\frac{\partial \bar{u}}{\partial \bar{r}}\right)_{r=1} = -i\Pi\alpha\frac{\sqrt{2}}{2}(1+i).$$

After keeping the real part of this derivative, we obtain:

$$2\pi\nu R\left(\frac{\partial u}{\partial r}\right)_{r=R} = 2\pi\nu R\frac{U_o}{R}\;\Pi\;\alpha\frac{\sqrt{2}}{2} \; = \pi\nu\alpha U_o\Pi \; = \sqrt{2\omega\nu}\;\frac{Q}{R}.$$

Here is the one-dimensional model for a low value of α:

$$\frac{\partial Q}{\partial x} + \frac{\partial S}{\partial t} \;\; = \;\; 0, \tag{26}$$

$$\frac{\partial Q}{\partial t} + \frac{\partial}{\partial x}\frac{Q^2}{S} \;\; = \;\; -\frac{S}{\rho}\frac{\partial p}{\partial x} + \sqrt{2\omega\nu}\;\frac{Q}{R}. \tag{27}$$

3.3 Conclusion.

Thanks to the "Womersley closure", we have determined the integral one-dimensional model. But to solve them, the system needs to be closed. For that, we introduce a pressure law $p = f(R)$ that includes specific properties of the wall.

4 Mechanic of Viscoelastic Wall

Now, let us focus on the tube wall.
Pulsated flows in flexible tubes can significantly deform its wall. It is depending on the amplitude of the pressure pulse. Deformations are determined by the material's properties.
Being in the prospect of applying our study to arterial flows, we attempt to formulate a pressure law that comes closer to the behaviour of a viscoelactic and non-linear material.

4.1 Deformation of Linear Elastic Tube and Wall Motion

We consider a linear elastic and isotropic walled tube with a constant wall thickness h, density ρ_w, Young's modulus E and Poisson's ratio ϑ.
A such material keep to the Hooke's Law (Fung, Humprey):

$$\overline{\overline{\varepsilon}} = \frac{1+\vartheta}{E}\,\overline{\overline{\sigma}} - \frac{\vartheta}{E}\,Tr(\overline{\overline{\sigma}})\overline{\overline{Id}},$$

where $\overline{\overline{\varepsilon}}$ is the strain tensor, and $\overline{\overline{\sigma}}$ the stress one.
Let $\overline{u} = (u_z, u_r, u_\varphi)$ be the the displacement of the wall. The strain tensor is defined by :

$$\overline{\overline{\varepsilon}} = \frac{1}{2}(\overline{\overline{Grad}}\,\overline{u} + \overline{\overline{Grad}}^{\,t}\,\overline{u}).$$

We are interesting in radial displacements u_r of the wall, and we do not take in account any displacement in axial direction u_z.
Let's write the Hooke's Law for the principal strain components:

$$\varepsilon_{zz} = \frac{1}{E}(\sigma_{xx} - \vartheta\,(\sigma_{rr} + \sigma_{\varphi\varphi})), \tag{28}$$

$$\varepsilon_{rr} = \frac{1}{E}(\sigma_{rr} - \vartheta\,(\sigma_{\varphi\varphi} + \sigma_{xx})), \tag{29}$$

$$\varepsilon_{\varphi\varphi} = \frac{1}{E}(\sigma_{\varphi\varphi} - \vartheta\,(\sigma_{xx} + \sigma_{rr})). \tag{30}$$

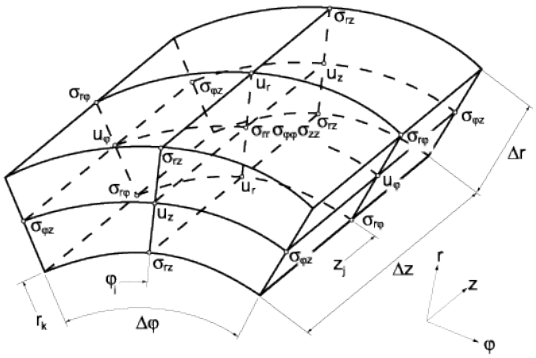

Figure 4: ***Stresses applied to the wall***
Internet Sources 2

As $u_z = 0$, then $\varepsilon_{zz} = 0$, and thus:

$$\sigma_{xx} = \vartheta\,(\sigma_{rr} + \sigma_{\varphi\varphi}). \tag{31}$$

We consider a small walled element with a circumference $d\varphi$ and a length dz. In radial and circumferential directions, strain components are given by:

$$\varepsilon_{\varphi\varphi} = \frac{\Delta\varphi}{R_o\, d\varphi} = \frac{(R_o + u_r)d\varphi - R_o\, d\varphi}{R_o\, d\varphi} \sim \frac{u_r}{R_o}.$$

By using the relationship (25):

$$\varepsilon_{\varphi\varphi} = \frac{1}{E}(\sigma_{\varphi\varphi} - \vartheta\ (\sigma_{xx} + \sigma_{rr})) = \sigma_{\varphi\varphi}\frac{(1-\vartheta^2)}{E} - \sigma_{rr}\frac{\vartheta(1+\vartheta)}{E}.$$

The tube is loaded with an internal pressure $p(z,t)$. In the linear elasticity theory of tubes, circumferential and radial stress components at the internal radius, are written :

$$\sigma_{rr} = -p, \tag{32}$$

$$\sigma_{\varphi\varphi} = p\frac{R_o^2 + (R_o+h)^2}{h(2R_o+h)}. \tag{33}$$

(See demonstration in Annexe 1)

Using these latest expression, it yields:

$$u_r = p\ \frac{R_o(1-\vartheta^2)}{E\ h}\left(\frac{R_o^2 + (R_o+h)^2}{2R_o+h} + \frac{h\ \vartheta}{1-\vartheta}\right).$$

The deformed radius is given by $R = R_o + u_r$. From this, we obtain the pressure loaded inside a linear elastic tube:

$$p = \kappa\ (R - R_o), \tag{34}$$

with

$$\kappa = \frac{E\ h}{R_o(1-\vartheta^2)}\frac{1}{\dfrac{R_o^2 + (R_o+h)^2}{2R_o+h} + \dfrac{h\ \vartheta}{1-\vartheta}}. \tag{35}$$

If we study the propagation in the case of thin wall ($h \to 0$), from the above formulation we find the "Copper Smith" formulation, or *la formule du "Chaudronnier"*, given by:

$$\kappa = \frac{E\ h}{R_o^2(1-\vartheta^2)}.$$

Nota Bene:

We can also write this elastic law by using the compliance of the tube C:

$$C = \frac{\partial S}{\partial p}.$$

This yields a pressure law given by $p = f(S - S_o)$.

4.2 Viscoelastic and Non-linear Behaviours

The will to apply this study to cardiovascular flows implies to consider solids with a viscoelastic behaviour. Indeed, when a pressure load is applied to a vascular tissue, the load-displacement curve is quite different from the unloading curve: this hysteresis

reveals a viscoelastic behaviour (Fung, Pedley, Jaffrin et *al.*, Von de Vosse et *al.*) .

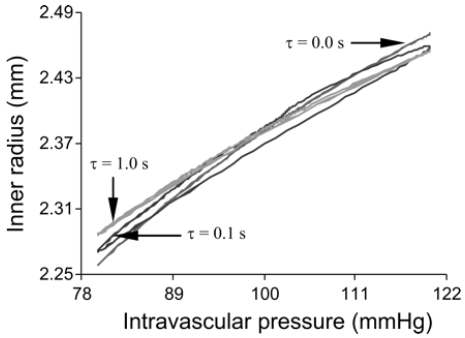

Figure 5: ***Hysteresis behaviour of the arterial wall***
This graph shows the viscoelastic and the non-linear behaviour of an artery wall Internet Source 3.

These materials have a time dependency in response to deformation.
If the stress time is below the characteristic relaxation time of the constitutive material, the components do not deform themselves, and we observe elastic effects (when stresses are proportional to deformation).
But if stress time is higher than the characteristic relaxation time, particles do deform themselves, and we observe a viscous response (when stresses are proportional to deformation's velocity).
These above curves coming from experimental data in Figure 5, show that vascular materials has non-linear behaviours.

4.2.1 A Linear Model: Kelvin-Voigt model

The simplest model of viscoelastic materials is linear and consist in adding elastic and viscous stresses:

$$\sigma = \sigma_{elastic} + \sigma_{viscous} = E\varepsilon + \eta\frac{\partial \varepsilon}{\partial t},$$

where E is a elasticity modulus, η a viscosity modulus, and ε the deformations.
This model has a graphic representation, which is a parallel line association of a spring and a piston: it is called the Kelvin Voigt model.

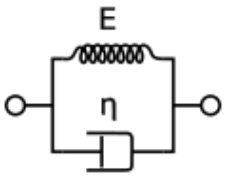

Figure 6: ***Kelvin-Voigt model***
Internet Source 4.

We are interesting in the radial deformation due to the pressure load inside a vis-

coelastic tube. So let us use the previous elastic law. It yields:

$$p = \kappa\,(R - R_o) + \eta\,\frac{\partial(R - R_o)}{\partial t}. \tag{36}$$

Nota Bene:
An other linear viscoelastic model widely used is the Maxwell model where:

$$\frac{1}{\eta}p + \frac{1}{E}\frac{\partial p}{\partial t} = \frac{\partial(R - R_o)}{\partial t}$$

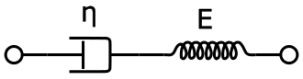

Figure 7: ***Maxwell model***
Internet Source 5.

4.2.2 A Non-Linear Model

Non- linear behaviours which are observed experimentally can be highlighted by adding a non-linear term in the previous linear viscoelastic model (Stergiopulos et *al.*, Tardy et *al.*, Horsten et *al.*). From now, we will use this following pressure law:

$$p = \kappa\,(R - R_o) + \eta\,\frac{\partial R}{\partial t} + \lambda(R - R_o)^2. \tag{37}$$

Nota Bene:

◇ Viscoelastic behaviour is also a property of Non-Newtonian fluids, like blood, which contents non negligible molecular chains of deformable particles. In a biomechanical study, we should consider a such fluid.

◇ Because of the complexity of some viscoelastic materials, it is not possible to define the different coefficients as can be done for Young's modulus in linear elasticity theory. But arbitrary values could be found thanks to experimental data.

4.3 Conclusion.

Having a simple model of closure (37), we are now able to solve the one-dimensional model formulated in [(24), (25)] for a small Wormersley number, or in [(26), (27)] with a large one.

5 Establishment of the Dimensionless Model of the Pressure Pulse Propagation

The aim of this section is to formulate the one-dimensional problem without dimension, and then introduce the numerical simulation methods.

5.1 Dimensional Problem

Before going further, we introduce some typical values in order to evaluate the non-dimensional parameters. We simulate the propagation of a pressure pulse $p(x=0,t) = P_o sin(\pi \frac{t}{T_o})$, with an entrance period T_o, and an amplitude P_o. The tube has a length of L_{tube}, a radius of R_o, and a thickness of h.

Let us remind the mathematical model:
Mass conservation:

$$\frac{\partial Q}{\partial x} + \frac{\partial S}{\partial t} = 0.$$

Momentum equation:

If $\alpha \to 0$,

$$\frac{\partial Q}{\partial t} + \frac{4}{3}\frac{\partial}{\partial x}\frac{Q^2}{S} = -\frac{S}{\rho}\frac{\partial p}{\partial x} - 8\,\nu\frac{Q}{R^2}.$$

If $\alpha \to \infty$,

$$\frac{\partial Q}{\partial t} + \frac{\partial}{\partial x}\frac{Q^2}{S} = -\frac{S}{\rho}\frac{\partial p}{\partial x} + \sqrt{2\omega\nu}\,\frac{Q}{R}.$$

Pressure law:

$$p = \kappa\,(R - R_o) + \eta\,\frac{\partial R}{\partial t} + \lambda(R - R_o)^2.$$

Moens-Korteveg velocity

We are interesting in the wave propagation. So a characteristic parameter of this motion is well the Moens-Korteveg velocity which is determined thanks to a wave equation. We obtain it by neglecting the viscous and the non-linear term in the momentum equation and the pressure law.

$$\frac{\partial Q}{\partial x} + \frac{\partial S}{\partial t} = 0. \tag{38}$$

$$\frac{\partial Q}{\partial t} + \frac{S}{\rho}\frac{\partial p}{\partial x} = 0. \tag{39}$$

$$p = \kappa\,(R - R_o). \tag{40}$$

We derive by the time (36) and by the space (37), and then subtract them:

$$\frac{\partial^2 S}{\partial t^2} + \frac{\partial}{\partial x}\frac{S}{\rho}\frac{\partial p}{\partial x} = 0. \tag{41}$$

We use variables defined by:$R = R_o(1 + \varepsilon\bar{r})$ and, $S = \pi R_o^2(1 + 2\varepsilon\bar{r})$ as a first-order development. $\bar{r}$ is a dimensionless variable for the radius.
By making a first-order approximation, the second term become:

$$S\;\partial p = \kappa\pi R_o^2(1 + 2\varepsilon\bar{r})R_o\;\partial(1 + \varepsilon\bar{r}) \approx \kappa\pi R_o^3\varepsilon\partial\bar{r}.$$

and then:

$$(2\pi R_o^2\varepsilon)\frac{\partial^2\bar{r}}{\partial t^2} + \frac{\kappa\pi R_o^3\varepsilon}{\rho}\frac{\partial^2\bar{r}}{\partial x^2} = 0.$$

Finally, we obtain the wave equation :

$$\frac{\partial^2 \bar{r}}{\partial t^2} + C_o^2 \frac{\partial^2 \bar{r}}{\partial x^2} = 0. \tag{42}$$

where C_o is the Moens-Korteveg velocity.

$$C_o = \sqrt{\frac{\kappa R_o}{2\rho}} \tag{43}$$

5.2 Non-dimensional Problem

Let come back to the one-dimensional problem, and use dimensionless variables defined by:

$$x = L_o\bar{x} \quad t = T_o\bar{t} \quad Q = Q_o\bar{Q} \quad R = R_o(1+\varepsilon\bar{r}) = R_o\bar{R} \quad S = \pi R_o^2(1+2\varepsilon\bar{r}) = \pi R_o^2\bar{S}.$$

Nota Bene:

The characteristic length of this model is different from L_{tube} as we are interesting in the wave propagation, and not the fluid motion.

Mass conservation:

$$\frac{Q_o}{L_o}\frac{\partial \bar{Q}}{\partial \bar{x}} + \frac{2\pi R_o^2 \varepsilon}{T_o}\frac{\partial \bar{r}}{\partial \bar{t}} = 0. \tag{44}$$

Momentum equation:

If $\alpha \to 0$,

$$\frac{\partial \bar{Q}}{\partial \bar{t}} + \frac{4}{3}\frac{T_o}{L_o}\frac{Q_o}{\pi R_o^2}\frac{\partial}{\partial \bar{x}}\left(\frac{\bar{Q}^2}{\bar{S}}\right) = -\frac{T_o}{Q_o}\frac{S}{\rho}\frac{\partial p}{\partial x} - 8\,\nu\frac{T_o}{R_o^2}\frac{\bar{Q}}{\bar{R}^2}. \tag{45}$$

If $\alpha \to \infty$,

$$\frac{\partial \bar{Q}}{\partial \bar{t}} + \frac{T_o}{L_o}\frac{Q_o}{\pi R_o^2}\frac{\partial}{\partial \bar{x}}\left(\frac{\bar{Q}^2}{\bar{S}}\right) = -\frac{T_o}{Q_o}\frac{S}{\rho}\frac{\partial p}{\partial x} + \sqrt{2\omega\nu}\,\frac{T_o}{R_o}\frac{\bar{Q}}{\bar{R}}. \tag{46}$$

Pressure law:

$$p = \kappa\,(R - R_o) + \eta\,\frac{\partial R}{\partial t} + \lambda(R - R_o)^2. \tag{47}$$

$\diamond$ *Pressure gradient term*:

$$S\frac{\partial p}{\partial x} = \kappa S\frac{\partial R}{\partial x} + \eta\,S\frac{\partial^2 R}{\partial x \partial t} + 2\,\lambda\,S(R - R_o)\frac{\partial R}{\partial x}$$
$$= \kappa\varepsilon\pi R_o^3(1+2\varepsilon\bar{r})\frac{\partial \bar{r}}{\partial x} + \eta\,\pi R_o^2(1+2\varepsilon\bar{r})\varepsilon R_o\frac{\partial^2 \bar{r}}{\partial x \partial t} + 2\,\lambda\,\pi R_o^2(1+2\varepsilon\bar{r})R_o\varepsilon\bar{r}\frac{\partial R_o\varepsilon\bar{r}}{\partial x}$$

After a first-order approximation, we have:

$$S\frac{\partial p}{\partial x} = \kappa\varepsilon\pi R_o^3\frac{\partial \bar{r}}{\partial x} + \eta\,\varepsilon\pi R_o^3\frac{\partial^2 \bar{r}}{\partial x \partial t} + \lambda\pi R_o^4\varepsilon^2\frac{\partial \bar{r}^2}{\partial x}$$

Derivative of the mass conservation equation (41) yields:
$$S\frac{\partial p}{\partial x} = \kappa\frac{\varepsilon\pi R_o^3}{L_o}\frac{\partial \bar{r}}{\partial \bar{x}} - \eta\ \frac{Q_o R_o}{2L_o}\frac{\partial^2 \bar{Q}}{\partial \bar{x}^2} + \lambda\frac{\pi R_o^4}{L_o}\varepsilon^2\frac{\partial \bar{r}^2}{\partial \bar{x}}$$

Let us use these latter results, and come back to the momentum equation:
If $\alpha \to 0$,

$$\frac{\partial \bar{Q}}{\partial \bar{t}} + \frac{4}{3}\frac{T_o\ Q_o}{L_o\ \pi R_o^2}\frac{\partial}{\partial \bar{x}}\left(\frac{\bar{Q}^2}{\bar{S}}\right) = -\varepsilon\frac{2\pi C_o^2 T_o R_o^2}{L_o Q_o}\frac{\partial \bar{r}}{\partial \bar{x}} + \eta\ \frac{T_o R_o}{2\rho L_o}\frac{\partial^2 \bar{Q}}{\partial \bar{x}^2} - \lambda\frac{\pi T_o R_o^4}{L_o Q_o \rho}\varepsilon^2\frac{\partial \bar{r}^2}{\partial \bar{x}} - 8\ \nu\frac{T_o}{R_o^2}\frac{\bar{Q}}{\bar{R}^2}.$$

If $\alpha \to \infty$,

$$\frac{\partial \bar{Q}}{\partial \bar{t}} + \frac{T_o\ Q_o}{L_o\ \pi R_o^2}\frac{\partial}{\partial \bar{x}}\left(\frac{\bar{Q}^2}{\bar{S}}\right) = -\varepsilon\frac{2\pi C_o^2 T_o R_o^2}{L_o Q_o}\frac{\partial \bar{r}}{\partial \bar{x}} + \eta\ \frac{T_o R_o}{2\rho L_o}\frac{\partial^2 \bar{Q}}{\partial \bar{x}^2} - \lambda\frac{\pi T_o R_o^4}{L_o Q_o \rho}\varepsilon^2\frac{\partial \bar{r}^2}{\partial \bar{x}} + \sqrt{2\omega\nu}\ \frac{T_o}{R_o}\frac{\bar{Q}}{\bar{R}}.$$

Two parameters, L_o and Q_o, are unknown.

$\diamond$ The same *reductio ad absurdum* gives the balance between terms of the mass conservation:
$$\frac{Q_o}{L_o} \sim \frac{2\pi R_o^2 \varepsilon}{T_o}, \tag{48}$$
and writing that the pressure gradient (without non-linear and viscous effect) is the driver of the propagation yields:
$$\varepsilon\frac{2\pi C_o^2 T_o R_o^2}{L_o Q_o} \sim 1. \tag{49}$$

Matching these above relationships gives:
$$\varepsilon \sim \frac{Q_o T_o}{L_o 2\pi R_o^2} \sim \frac{L_o Q_o}{2\pi C_o^2 T_o R_o^2}$$

And finally:
$$L_o = C_o T_o. \tag{50}$$
$$\varepsilon = \frac{Q_o}{2\pi C_o R_o^2} \tag{51}$$

$\diamond$ The size order of the rate flow is giver by the amplitude of the inlet pressure P_o. Basically we have:
$$\frac{T_o}{Q_o}\ Scale\left(\frac{S}{\rho}\frac{\partial p}{\partial x}\right) \sim \frac{T_o}{Q_o}\frac{\pi R_o^2 P_o}{\rho L_o} \sim 1$$
So we suppose that:
$$Q_o = \frac{\pi R_o^2 P_o}{\rho C_o} \tag{52}$$

Finally, we have to solve :

Mass conservation:
$$\frac{\partial \bar{Q}}{\partial \bar{x}} + \frac{\partial \bar{r}}{\partial \bar{t}} = 0. \tag{53}$$

Momentum equation:

If $\alpha \to 0$,

$$\frac{\partial \bar{Q}}{\partial \bar{t}} + \varepsilon_1 \frac{4}{3} \frac{\partial}{\partial \bar{x}} \left(\frac{\bar{Q}^2}{\bar{S}} \right) = -\frac{\partial \bar{r}}{\partial \bar{x}} + \eta \, \varepsilon_{klv} \frac{\partial^2 \bar{Q}}{\partial \bar{x}^2} - \lambda \varepsilon_{nl} \frac{\partial \bar{r}^2}{\partial \bar{x}} - \frac{16\pi}{\alpha^2} \frac{\bar{Q}}{\bar{R}^2}. \tag{54}$$

If $\alpha \to \infty$,

$$\frac{\partial \bar{Q}}{\partial \bar{t}} + \varepsilon_1 \frac{\partial}{\partial \bar{x}} \left(\frac{\bar{Q}^2}{\bar{S}} \right) = -\frac{\partial \bar{r}}{\partial \bar{x}} + \eta \, \varepsilon_{klv} \frac{\partial^2 \bar{Q}}{\partial \bar{x}^2} - \lambda \varepsilon_{nl} \frac{\partial \bar{r}^2}{\partial \bar{x}} + \frac{\pi \sqrt{8}}{\alpha} \frac{\bar{Q}}{\bar{R}}. \tag{55}$$

With

$$\varepsilon_1 = \frac{Q_o}{C_o \, \pi R_o^2} \quad \varepsilon_{klv} = \frac{R_o}{2\rho C_o} \quad \varepsilon_{nl} = \frac{Q_o}{4\pi\rho \, C_o^3}$$

In this system of equations, all the variables and small parameters ε_1, $\eta\varepsilon_{klv}$ and $\lambda\varepsilon_{nl}$ are without dimensions.
We can now establish a numerical method to solve it.

5.3 Numerical Method

To solve the problem, the numerical solutions are computed with the MacCormack scheme which is a predictor-corrector technical (Fullana J.M.). It is three-point in space, two-level in time and it is second order accurate in time and in space.
Here is the principle of this method which is particularly well adapted to first-order hyperbolic problem:

$$\frac{\partial \mathbf{V}}{\partial t} + \frac{\partial \mathbf{F}}{\partial x} + \mathbf{S} = 0, \tag{56}$$

where $\mathbf{V}$ is the vector of dynamical variables, $\mathbf{F}$ is vector conserved quantities and $\mathbf{S}$ is the source term.

$\diamond$*Predictor step*

$$\mathbf{V}_i^* = \mathbf{V}_i^n - \frac{\Delta t}{\Delta x}(\mathbf{F}_{i+1}^n - \mathbf{F}_i^n) + \Delta t \, \mathbf{S}_i^n \tag{57}$$

$\diamond$*Corrector step*

$$\mathbf{V}_i^{n+1} = \frac{1}{2}(\mathbf{V}_i^n + \mathbf{V}_i^*) - \frac{\Delta t}{2 \, \Delta x}(\mathbf{F}_i^* - \mathbf{F}_{i-1}^*) + \Delta t \, \mathbf{S}_i^* \tag{58}$$

In our momentum equation, we have a dissipative term that will be computed with the second-order cell-centrered scheme.

The subscript i represents space iterations, and $0 \leq i \leq n_x$, with $n_x = 500$. Thus the space-step is given by $\Delta x = \dfrac{L_{tube}/L_o}{n_x} \approx 0.0124$.
The superscript n represent time iteration, and can go as long as we need to follow the wave propagation. We set the time-step to $\Delta t = 0.001$.
We note that the CFL condition *(Courant-Friedrichs-Lewy condition)* $\dfrac{\Delta t}{\Delta x} \leq 1$ is obeyed.

Using this method we write the algorithm with the C language.)

Boundary and initial conditions .

Every variable is set to zero at t=0.

We impose at the entrance $p(x = 0, t) = Po\ sin(\pi \frac{t}{To})$. The problem's variables are $\bar{Q}$ and $\bar{r}$, so the inlet condition is setting after solving a second-degree equation in $\bar{r}(x = 0)$, coming from the pressure law.

All others inlet and outlet boundary conditions using a secon-order cell-centered scheme.

(See the full algorithm in Annexe.2)

Conclusion.

Before applying our analysis, we will focus in the following section on each term of the one-dimensional model.

6 Influence of the Parameters on the Moving Wave

We want to realise how the viscous and the non-linear terms of the pressure law contribute to the pulse propagation.
We start from the system of dimensionless equations [(52),(53),(54)]

6.1 Viscous Wall Damping: Kelvin Voigt model

We first take into account the viscous wall damping coming from the Kelvin Voigt model. So we neglect the fluid viscosity, and the both wall and fluid non linearities.

$$\begin{cases} \dfrac{\partial \bar{Q}}{\partial \bar{x}} + \dfrac{\partial \bar{r}}{\partial \bar{t}} = 0 \\ \dfrac{\partial \bar{Q}}{\partial \bar{t}} = -\dfrac{\partial \bar{r}}{\partial \bar{x}} + \eta\, \varepsilon_{klv} \dfrac{\partial^2 \bar{Q}}{\partial \bar{x}^2} \end{cases}$$

Using the mass conservation equation gives:

$$\begin{cases} \dfrac{\partial \bar{Q}}{\partial \bar{x}} + \dfrac{\partial \bar{r}}{\partial \bar{t}} = 0 \\ \dfrac{\partial \bar{Q}}{\partial \bar{t}} = -\dfrac{\partial \bar{r}}{\partial \bar{x}} - \eta\, \varepsilon_{klv} \dfrac{\partial^2 \bar{r}}{\partial \bar{x} \partial \bar{t}} \end{cases}$$

As the wall viscosity is small, it takes long before creating a noticeable effect. So we introduce a multi-scale expansion in order to see the effect of small dissipation. As we have noticed, the wave moves at the Moens Korteweg velocity C_o. So we choose as space variable $\xi = x - C_o\, t$, and $\bar{\xi} = \bar{x} - \bar{t}$ without dimension. We choose $\bar{\tau} = \eta\, \varepsilon_{klv} \bar{t}$. That means that $\bar{t}$ is a long time behaviour compared to $\bar{\tau}$.
Let us use these above change of variables. The chain rule derivatives give:

$$\frac{\partial}{\partial \bar{x}} = \frac{\partial \bar{\xi}}{\partial \bar{x}} \frac{\partial}{\partial \bar{\xi}} + \frac{\partial \bar{\tau}}{\partial \bar{x}} \frac{\partial}{\partial \bar{\tau}} \quad and \quad \frac{\partial}{\partial \bar{t}} = \frac{\partial \bar{\xi}}{\partial \bar{t}} \frac{\partial}{\partial \bar{\xi}} + \frac{\partial \bar{\tau}}{\partial \bar{t}} \frac{\partial}{\partial \bar{\tau}},$$

so,

$$\frac{\partial}{\partial \bar{x}} = \frac{\partial}{\partial \bar{\xi}} \quad and \quad \frac{\partial}{\partial \bar{t}} = -\frac{\partial}{\partial \bar{\xi}} + \eta\, \varepsilon_{klv} \frac{\partial}{\partial \bar{\tau}},$$

and the system becomes:

$$\begin{cases} \dfrac{\partial \bar{Q}}{\partial \bar{\xi}} - \dfrac{\partial \bar{r}}{\partial \bar{\xi}} + \eta\, \varepsilon_{klv} \dfrac{\partial \bar{r}}{\partial \bar{\tau}} = 0 \\ -\dfrac{\partial \bar{Q}}{\partial \bar{\xi}} + \dfrac{\partial \bar{r}}{\partial \bar{\xi}} + \eta\, \varepsilon_{klv} \left(\dfrac{\partial \bar{Q}}{\partial \bar{\tau}} - \dfrac{\partial^2 \bar{r}}{\partial \bar{\xi}^2} \right) + (\eta\, \varepsilon_{klv})^2 \dfrac{\partial^2 \bar{r}}{\partial \bar{\xi} \partial \bar{\tau}} = 0 \end{cases}$$

We take an asymptotic expansion for the flux and the perturbation of the radius which depend on these new variables:

$$\bar{Q}(\bar{x}, \bar{t}) = \bar{Q}_1(\bar{\xi}, \bar{\tau}) + \eta\, \varepsilon_{klv} \bar{Q}_2(\bar{\xi}, \bar{\tau}) + ...$$
$$\bar{r}(\bar{x}, \bar{t}) = \bar{r}_1(\bar{\xi}, \bar{\tau}) + \eta\, \varepsilon_{klv} \bar{r}_2(\bar{\xi}, \bar{\tau}) + ...$$

Introducing this expansion into the motion equation gives:

$$\begin{cases} \dfrac{\partial \bar{Q}_1}{\partial \bar{\xi}} - \dfrac{\partial \bar{r}_1}{\partial \bar{\xi}} + \eta\, \varepsilon_{klv} \left(\dfrac{\partial \bar{r}_1}{\partial \bar{\tau}} + \dfrac{\partial \bar{Q}_2}{\partial \bar{\xi}} - \dfrac{\partial \bar{r}_2}{\partial \bar{\xi}} \right) + ... = 0 \\ -\dfrac{\partial \bar{Q}_1}{\partial \bar{\xi}} + \dfrac{\partial \bar{r}_1}{\partial \bar{\xi}} + \eta\, \varepsilon_{klv} \left(\dfrac{\partial \bar{Q}_1}{\partial \bar{\tau}} - \dfrac{\partial^2 \bar{r}_1}{\partial \bar{\xi}^2} - \dfrac{\partial \bar{Q}_2}{\partial \bar{\xi}} + \dfrac{\partial \bar{r}_2}{\partial \bar{\xi}} \right) + ... = 0 \end{cases}$$

At the order $(\eta\ \varepsilon_{klv})^0$, we observe that $\bar{r}_1 = \bar{Q}_1 + \phi(\bar{\tau})$ is a solution of the problem. The function $\phi(\bar{\tau})$ is unknown, and we choose a constant one $\phi(\bar{\tau}) = 0$, as the initial condition could only be $\phi(0) = 0$. The system becomes:

$$\begin{cases} \dfrac{\partial \bar{r}_1}{\partial \bar{\tau}} + \dfrac{\partial \bar{Q}_2}{\partial \bar{\xi}} - \dfrac{\partial \bar{r}_2}{\partial \bar{\xi}} + ... = 0 \\ \dfrac{\partial \bar{Q}_1}{\partial \bar{\tau}} - \dfrac{\partial^2 \bar{r}_1}{\partial \bar{\xi}^2} - \dfrac{\partial \bar{Q}_2}{\partial \bar{\xi}} + \dfrac{\partial \bar{r}_2}{\partial \bar{\xi}} + ... = 0 \end{cases},$$

and when we add these above order $(\eta\ \varepsilon_{klv})$ equations, it gives:

$$\frac{\partial \bar{r}_1}{\partial \bar{\tau}} + \frac{\partial \bar{Q}_1}{\partial \bar{\tau}} - \frac{\partial \bar{r}_1^2}{\partial \bar{\xi}^2} = 0.$$

As $\bar{r}_1 = \bar{Q}_1$, then :

$$\frac{\partial \bar{r}_1}{\partial \bar{\tau}} = \frac{1}{2} \frac{\partial^2 \bar{r}_1}{\partial \bar{\xi}^2} \tag{59}$$

Its solution is the solution of *heat equation* with $\frac{1}{2}$ as a coefficient of diffusion.

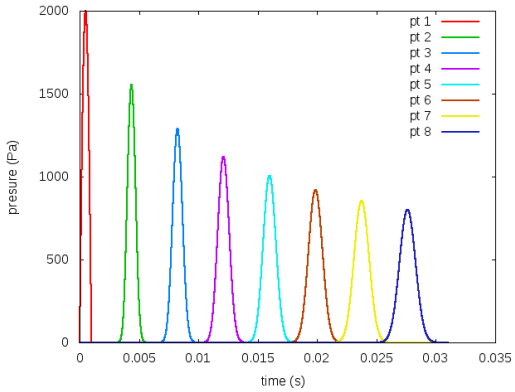

Figure 8: ***Displacement and diffusion of a diffusive wave***: A pressure pulse propagation is observed at different points along the tube as a function a of time. This moving wave shows the viscous effect due only to the wall's material. Viscoelasticity creates diffusion of the pulse when it is also observed its spreading

6.2 Non Linear Wall Stiffening

We take into account the non-linear wall stiffening, so we neglect the both wall and fluid viscosity, and fluid non linearities.

$$\begin{cases} \dfrac{\partial \bar{Q}}{\partial \bar{x}} + \dfrac{\partial \bar{r}}{\partial \bar{t}} = 0 \\ \dfrac{\partial \bar{Q}}{\partial \bar{t}} = -\dfrac{\partial \bar{r}}{\partial \bar{x}} - \lambda \varepsilon_{nl} \dfrac{\partial \bar{r}^2}{\partial \bar{x}} \end{cases}$$

Like previously, we introduce a multi-scale expansion in order to see the effect of small non linearities, and we use these following dimensionless variable:

$$\bar{\xi} = \bar{x} - \bar{t} \quad and \quad \bar{\tau} = \lambda\ \varepsilon_{nl} \bar{t}.$$

It yields the chain rule derivative:

$$\frac{\partial}{\partial \bar{x}} = \frac{\partial}{\partial \bar{\xi}} \quad and \quad \frac{\partial}{\partial \bar{t}} = -\frac{\partial}{\partial \bar{\xi}} + \lambda\, \varepsilon_{nl} \frac{\partial}{\partial \bar{\tau}},$$

We proceed like previously by looking for

$$\bar{Q}(\bar{x}, \bar{t}) = \bar{Q}_1(\bar{\xi}, \bar{\tau}) + \lambda\, \varepsilon_{nl} \bar{Q}_2(\bar{\xi}, \bar{\tau}) + ...$$

and

$$\bar{r}(\bar{x}, \bar{t}) = \bar{r}_1(\bar{\xi}, \bar{\tau}) + \lambda\, \varepsilon_{nl} \bar{r}_2(\bar{\xi}, \bar{\tau}) + ...$$

Introducing this expansion into the motion equation gives:

$$\begin{cases} \dfrac{\partial \bar{Q}_1}{\partial \bar{\xi}} - \dfrac{\partial \bar{r}_1}{\partial \bar{\xi}} + \lambda\, \varepsilon_{nl} \left(\dfrac{\partial \bar{r}_1}{\partial \bar{\tau}} + \dfrac{\partial \bar{Q}_2}{\partial \bar{\xi}} - \dfrac{\partial \bar{r}_2}{\partial \bar{\xi}} \right) + ... = 0 \\ -\dfrac{\partial \bar{Q}_1}{\partial \bar{\xi}} + \dfrac{\partial \bar{r}_1}{\partial \bar{\xi}} + \lambda\, \varepsilon_{nl} \left(\dfrac{\partial \bar{Q}_1}{\partial \bar{\tau}} + \dfrac{\partial \bar{r}_1^2}{\partial \bar{\xi}} - \dfrac{\partial \bar{Q}_2}{\partial \bar{\xi}} + \dfrac{\partial \bar{r}_2}{\partial \bar{\xi}} \right) + ... = 0 \end{cases}$$

We note that $\bar{r}_1 = \bar{Q}_1$ is a solution of the problem at order $(\lambda\, \varepsilon_{nl})^0$. So at the next order we have:

$$\begin{cases} \dfrac{\partial \bar{r}_1}{\partial \bar{\tau}} + \dfrac{\partial \bar{Q}_2}{\partial \bar{\xi}} - \dfrac{\partial \bar{r}_2}{\partial \bar{\xi}} + ... = 0 \\ \dfrac{\partial \bar{Q}_1}{\partial \bar{\tau}} + \dfrac{\partial \bar{r}_1^2}{\partial \bar{\xi}} - \dfrac{\partial \bar{Q}_2}{\partial \bar{\xi}} + \dfrac{\partial \bar{r}_2}{\partial \bar{\xi}} + ... = 0 \end{cases},$$

After a substitution, and as $\bar{r}_1 = \bar{Q}_1$, this yields:

$$\frac{\partial \bar{r}_1}{\partial \bar{\tau}} + \frac{1}{2} \frac{\partial \bar{r}_1^2}{\partial \bar{\xi}} = 0.$$

Or,

$$\frac{\partial \bar{r}_1}{\partial \bar{\tau}} + \bar{r}_1 \frac{\partial \bar{r}_1}{\partial \bar{\xi}} = 0, \tag{60}$$

of which the solution is the one of an *advection equation*.

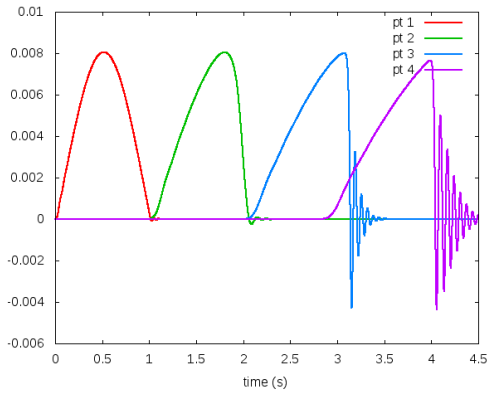

Figure 9: ***Displacement and stiffening of a flood wave:*** A pressure pulse propagation is observed at different points along the tube. This moving wave shows the non-linear effect only due to the wall's material. Non linearity creates stiffening of the pulse. The amplitude of the pressure pulse is not affected by non-linearities. The instabilities are due to the impossibility for the code to compute the choc.

6.3 Conclusion.

We have paid attention to the contribution of each terms of the model in the moving wave. Its effects are different when are tuning the parameters. We are now able to quantify these different parameters, and simulate properly a wave propagation in a viscoelastic and non-linear tube.

7 One-dimensional Model compared with Two-dimensional Axisymmetrical Model.

7.1 Simulation of Wave Propagations with COMSOL 3.4

To realize how much the one-dimensional model is close to the full Navier-Stokes model, we use the multi-physic software COMSOL 3.4. The latter is able to built model for fluid or solid motions which are affected by a solid-fluid coupling.

The structural mechanics computations are done using a 2D axially symmetric stress-strain formulation. The material is presumed to be linear and elastic.
The fluid flow is described by the Navier-Stokes equations [(1),(2),(3)] previously written.
A Moving Mesh application mode allows to simulate tube's deformations driven by the fluid motion in a deforming geometry configuration.

7.1.1 Model Definition.

The model is set up in 2D axial symmetry (See Figure 10). An viscoelastic tube of length $L_{tube} = 0.08\ m$, inner radius $R_0 = 0.002\ m$, and outer radius 0.003 m, contains water of density $\rho = 1000\ kg.m^{-3}$ and viscosity $\mu = 10^{-6}\ Pa.s$. A pressure pulse is applied at the entrance of the tube $p(z = 0, t) = Po\ sin(\pi \frac{t}{T_o})$, where the period is set to $T_o = 1\ ms$, and the pressure amplitude is $P_o = 2,0.10^3\ Pa$. We observe the wave propagation and the tube deformations during seven periods.

The elastic behaviour is defined in material properties by setting arbitrary value of Young's modulus $E = 1,0.10^6\ Pa$ and Poisson's ratio $\vartheta = 0.33$.
The viscous behaviour is provided by the Rayleigh damping model which describe the solid motion with viscous damping and with a single degree of freedom by:

$$m\frac{d^2u}{dt^2} + \xi\frac{du}{dt} + ku = f(t), \tag{61}$$

where u is the displacement, ξ is the damping parameter, m the mass, and k the stiffness coefficient.
And the damping parameter is expressed by:

$$\xi = \alpha_{dM}.m + \beta_{dK}.k \tag{62}$$

It has been automatically set in COMSOL $\alpha_{dM} = 1s^{-1}$ and $\beta_{dK} = 0.001s$.

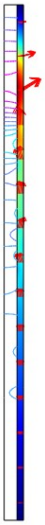

Figure 10: ***Geometry of the viscoelastic tube which is deforming under the pressure pulse***: Arrows represent deformations of the wall, stream lines is the pressure inside the tube, and isosurfaces are the total displacement

7.1.2 Boundary Condition.

The both ends of the tube are fixed, and the outlet flow is set to no normal stress. The entrance has a outlet type boundary set to a pressure condition. A inlet type boundary for a pressure condition shows numerical instabilities. (See Figure 11).

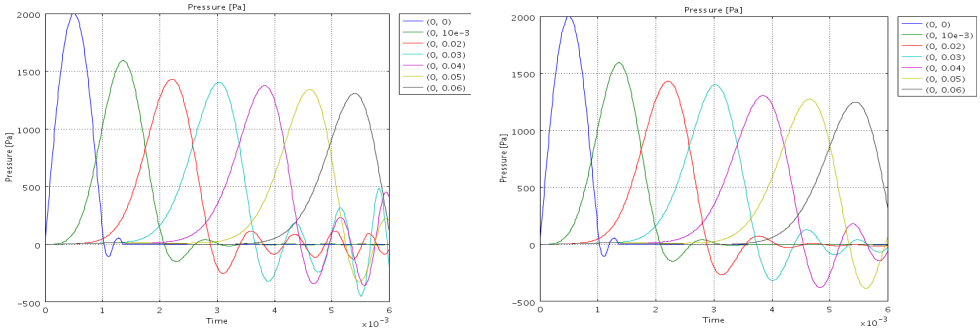

Figure 11: ***Instabilities due to a inlet type boundary condition at the entrance***: On the left is the result of a simulation with a inlet type boundary, and on the right with a outlet type.

Fluid and moving mesh boundary conditions at the fluid-solid interface are the velocity and displacement variables of the solid.
The axis has a symmetrical type boundary set to a axisymmetrical condition.

7.1.3 Results.

Numerical solutions depend on the fineness and the shape of meshing. A comparison of several meshing allows us to keep the one with the fewest numerical errors.
Also, we might have not get the best solution that COMSOL 3.4 could provide since the more meshes are fine, the more computing solutions needs power and time.

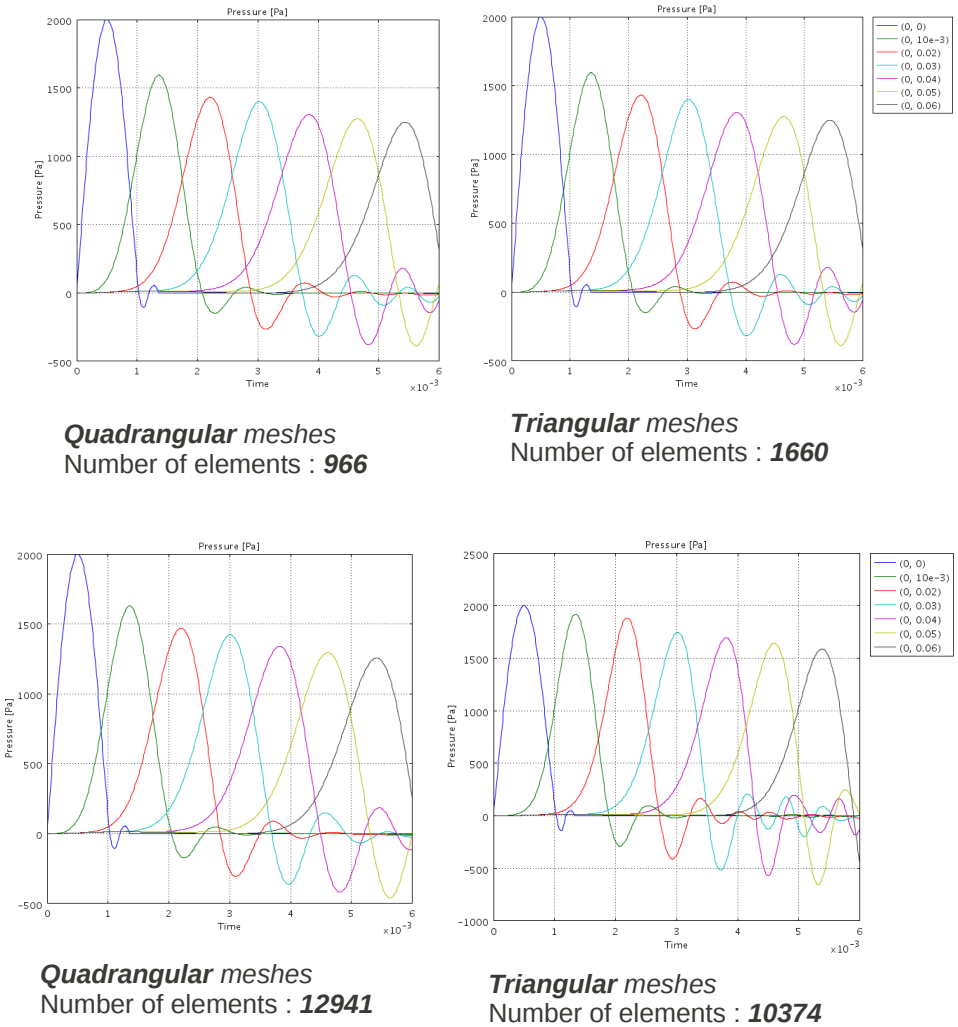

Figure 12: ***Comparison between several meshings.***

We note that there are not obvious differences when we refine the quadrangular meshes. We see by the triangular meshing that a coarse one diffuses numerically the solution. And when we compare the both finer triangular and quadrangular meshing, we note that the quadrangular's one diffuse also the solution.
So we will use the finer triangular meshing to study the one-dimensional model.

7.2 Comparison with the One-Dimensional model.

A such configuration gives as Womersley number $\alpha = 158.5$, and implies to use the model in the case of $\alpha \to \infty$. The Reynolds number is $Re = \frac{U_o}{\omega R_o}\alpha^2$. The characteristic value of the pressure P_o could be given by $\frac{P_o}{\rho U_o^2} \sim 1$..

So $Re = \sqrt{\frac{P_o}{\rho}}\frac{1}{\omega R_o}\alpha^2$, and $Re = 2,8.10^3$.

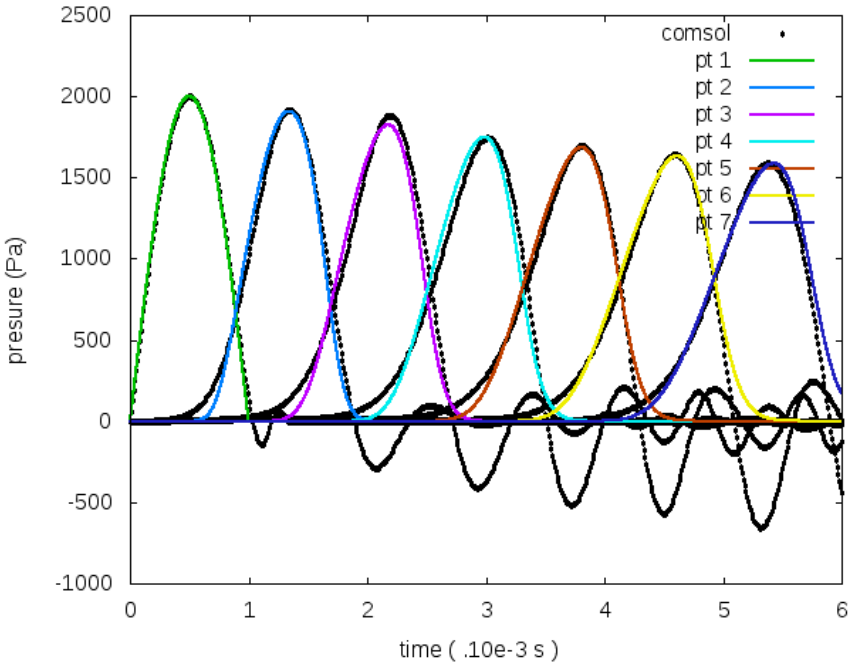

Figure 13: ***Comparison of Wave Propagation Simulation between COMSOL and the One-dimensional Model.***: *Results of the 1D simulation are plotted with color when the COMSOL's ones are in black. It is plotted the internal pressure wave of the tube at seven points with intervals of 0.01 meters. We had not checked if the instabilities that appear is physical or numerical. But dispersive properties show similar behaviours. Dispersion would have been formulated by adding a second order derivative of the radius in the solid behaviour.*

Using the theoretical expressions of the Moens-Korteweg velocity and the elastic coefficient κ gives a wave that propagates faster than the COMSOL's one which is $12,9\ m.s^{-1}$. We can suppose that the κ coefficient coming from the only linear elastic behaviour of the tube (and so the Moens-Kortevag velocity), is not appropriate to a viscoelastic and non-linear tube.
As C_o is proportional to $\sqrt{E}$, we have decreased the Young modulus initially set to $1,0.10^6\ Pa$, to $E = 0,69.10^6\ Pa$ in order to get the same propagation velocity than

COMSOL.

Otherwise, the pressure law used in the one-dimensional model shows a viscous coefficient η and a non-linear coefficient λ, which are not defined. Having displayed the contribution to the the moving wave of the both viscous wall damping and non-linear wall stiffening, we are able to approximate the non-linear and viscous coefficients thanks to the COMSOL 3.4 computation.
We get closer to the COMSOL wave propagation by setting in the one-dimensional model these following values:

$$\lambda = -1,32.10^{12}\ kg \cdot m^{-3} \cdot s^{-2} \quad and \quad \eta = 1,88.10^{5}\ kg \cdot m^{-3} \cdot s^{-1}$$

Using expressions of ε_{klv} and ε_{nl} defined in the section 4.1, we estimate in the moving wave the rate of the viscous wall damping at $\eta\varepsilon_{klv} = 1.5$ %, and the rate of the non-linear wall stiffening at $\lambda\varepsilon_{nl} = 9.5$ %.

This computation asserts that the viscoelastic behaviour of the tube is not a dominating factor in the observed damping: the rate of the viscous fluid damping is $\frac{\pi\sqrt{8}}{\alpha} = 5,6\ \% > \eta\varepsilon_{klv}$. But the non-linear behaviour of the wall is. Indeed, the rate of the non-linear fluid stiffening is $\varepsilon_1 = 1,2\% < \lambda\varepsilon_{nl}$.

7.3 Conclusion.

The comparison between the COMSOL 3.4 simulation and the one-dimensionnal model asserts that a such model is a good alternative to the use of the full 3D Navier-Stokes equation.
Let us now see how much that one-dimensional model comes closer to measurement datas.

8 One-dimensional Model compared with an Experiment.

8.1 Experimental Model

The experiment consists in analysing the propagation of a pulsatile wave into three kinds of viscoelastic tubes (natural rubber, silicone, and neoprene rubber), of which the length is $L_{tube} = 35.15\ m$, the radius $R_o = 4\ mm$, and the thickness $h = 2\ mm$. The fluid is water ($\rho = 10^3\ kg.m^{-3}$), and the input flow velocity waveform is a half cycle of a sinusoidal wave. The period is $T_o = 0.3\ s$ and the total input flow volume is $V_o = 4.5\ ml$.
The inner pressure wave is measured in each tube with intervals of 5 *meters* using a pressure sensor.

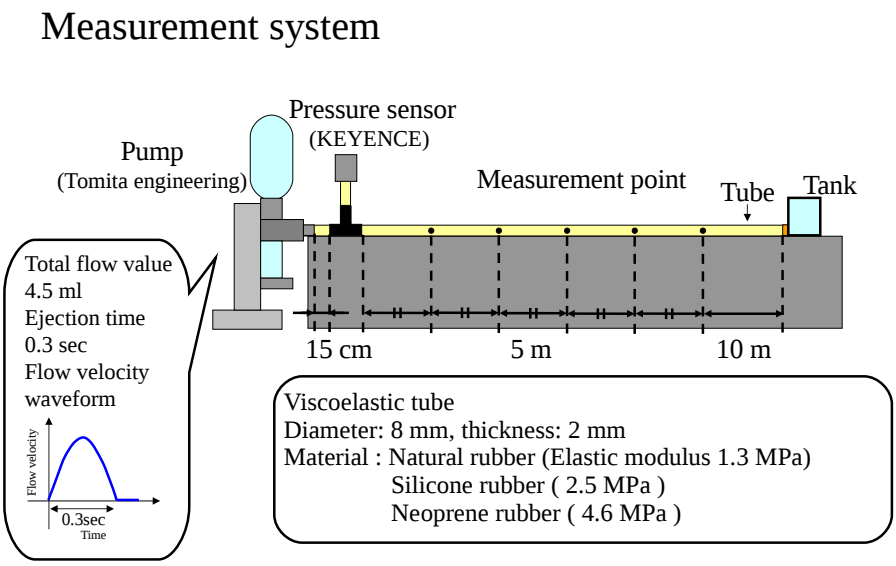

Figure 14: ***Measurement system of the experiment carried out by M. Saito.***

8.2 Numerical method

The numerical method is exactly the same which as been introduced in section 4. Contrary to the COMSOL simulation, here is imposed the inlet rate of flow $Q(x = 0, t) = Q_o\ sin(\pi \frac{t}{To})$. Indeed,

$$V_o = \int_{t=0}^{t=T_o} Q_o\ sin(\pi \frac{t}{T_o})\ dt = 2Q_o \frac{T_o}{\pi}.$$

So we defined inlet the rate of flow amplitude by:

$$Q_o = \frac{\pi V_o}{2T_o}.$$

8.3 Results

The below figures show the comparison between different kind of viscoelastic tubes and the one-dimensional model, and gives the different parameter used for the computation.

A such configuration gives $\alpha = 18.3$ as Womersley number, and implies to use the model in the case of $\alpha \rightarrow 0$.The Reynolds number is $Re = \frac{U_o}{\omega R_o}\alpha^2$. The characteristic value the rate of flow gives the one of the flow velocity. Indeed, $Q_o = \pi R_o^2 U_o$.
So $Re = \frac{Q_o}{\pi\omega R_o^3}\alpha^2$. And as $Q_o = \frac{\pi V_o}{2T_o}$ and $\omega = \frac{2\pi}{T_o}$, this yields $Re = \frac{V_o}{4\pi R_o^3}\alpha^2$. Finally $Re = 7,5$.

The Poisson's ration is close to $\vartheta = 0.5$ for each material.

It has been determined experimentaly a Young's modulus E_{exp} for each material. Like the previous comparison, using the theoretical expression of the elastic coefficient κ gives a wave that propagates, excepted silicone, faster than the experimental one. We had to decrease this value for the natural and neoprene rubber in order to find the appropriate propagation velocity.

The input parameters of the experiment (V_o and T_o) does not allow to reproduce properly the inlet pressure pulse .It seems that the input value of V_o needs to be set in the code with a higher one than the experiment. Setting $V_o = 5.1\ ml$ for each computation gives an appropriate pressure entrance.

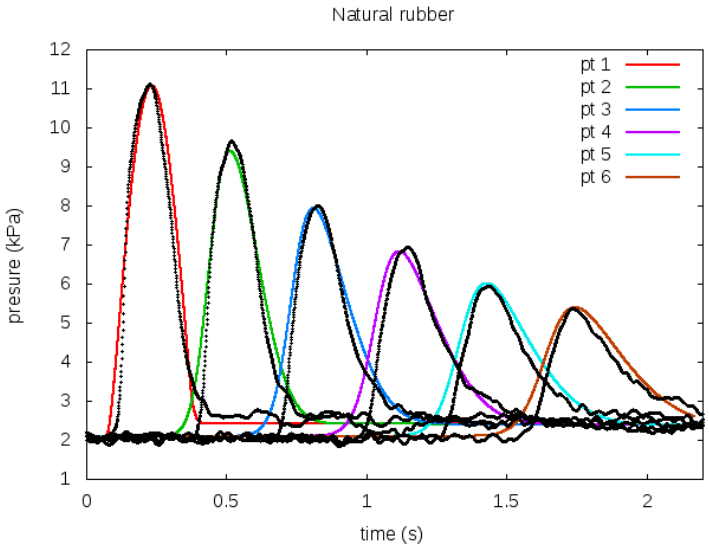

Figure 15: ***Natural rubber results***:
$E_{exp} = 1,3.10^6\ Pa$,
$E = 0,8.10^6\ Pa,\ \varepsilon = 1,6\%,\ \varepsilon_1 = 3,1\ \%$
$\lambda = 0,4.10^{12},\ \eta = 2,3.10^6,\ \lambda\varepsilon_{nl} = 25,1\ \%,\ \eta\varepsilon_{klv} = 3.7\ \%$.

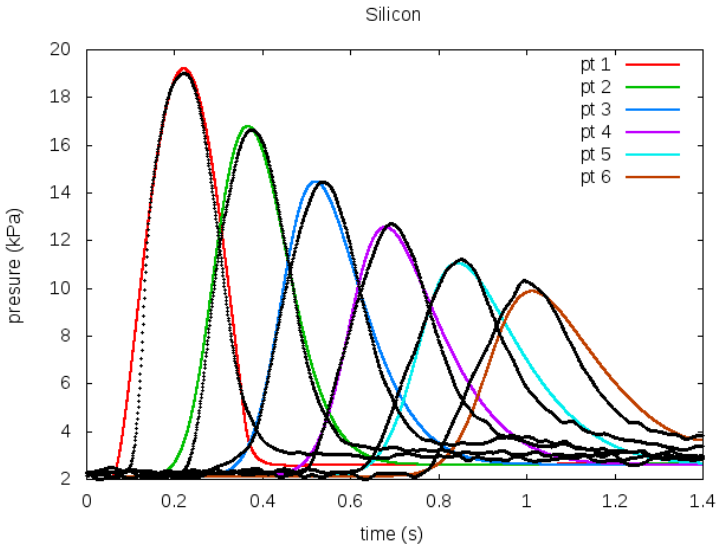

Figure 16: ***Silicone results***:
$E_{exp} = 2,5.10^6\ Pa$,
$E = 2,5.10^6\ Pa,\ \varepsilon = 1,0\ \%,\ \varepsilon_1 = 2,0\ \%,$
$\lambda = 4,0.10^{12},\ \eta = 24,0.10^6,\ \lambda\varepsilon_{nl} = 47,8\ \%,\ \eta\varepsilon_{klv} = 6.9\ \%.$

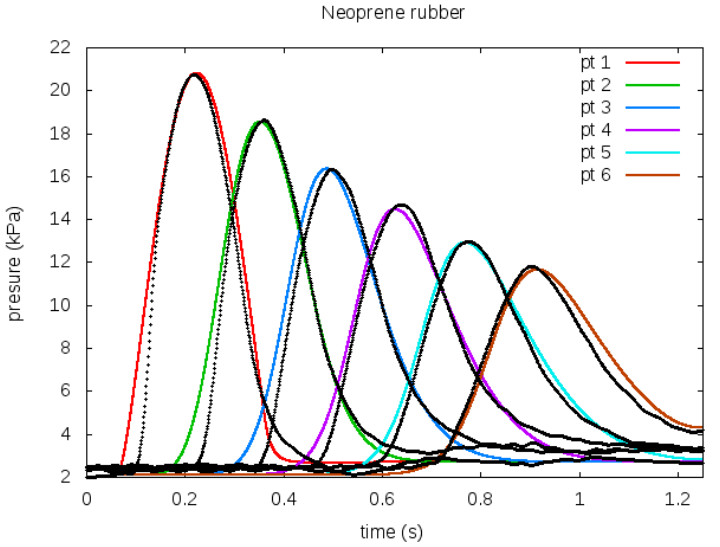

Figure 17: ***Neoprene rubber results:***
$E_{exp} = 4,6.10^6\ Pa$,
$E = 3,45.10^6\ Pa,\ \varepsilon = 0,9\ \%,\ \varepsilon_1 = 1,7\ \%,$
$\lambda = 5,0.10^{12},\ \eta = 29,5.10^6,\ \lambda\varepsilon_{nl} = 35,5\ \%,\ \eta\varepsilon_{klv} = 6.2\ \%.$

Viscous and a non-linear coefficients η and λ has been determined thanks to their obvious contribution to the moving wave behaviour. Using the fixed coefficient ε_{nl} and ε_{klv} given in the section 5.2, we can estimate in the moving wave the rate of the viscous wall damping $\eta\varepsilon_{klv}$, and the rate of the non-linear wall stiffening $\lambda\varepsilon_{nl}$.

We have also estimated the rate of the fluid non-linearity ε_1.
The Womersley number is fixed and gives for the three wave propagations the rate of the viscous fluid damping:

$$\frac{16\pi}{\alpha^2} = 15,0\ \%.$$

8.4 Concluding discussion.

For the three kinds of tube, the one-dimensional model shows a damping and non linearities in the same order of magnitude that the measurements.
Looking the rate of the viscous wall damping beside the fluid's one asserts that the viscoelasticity of the wall is a predominant behaviour in the observed wave propagation.

A better agreement might have be found if the inlet conditions in the simulation had been exactly the same as the input parameters of the experiment.

However, the method used to fit the curves seems to be interesting to determine material's coefficient. Indeed, we could restart these measurements with the same tubes, but with an other fluid of which the viscosity is well known. That could quantify the efficiency of a such method.
In our case, it is encouraging to find different cofficient for each material.

9 Opening on Biomechanical issues

We propose to simulate the propagation of a pressure pulse in a "viscoelastic aneurysm". This computation gives a preview on the becoming of the arterial pressure in the case of aneurysm, and helps to quantify how alarming could be this disease.

Like previously, we compute with COMSOL Multiphysics 3.4. The geometry is built from the tube's one. We first extrude a part of the wall, and then create well set up points that allow to plot the "aneurysm". This latest is plotted thanks to a Bezier curve (Ritzenthaler).

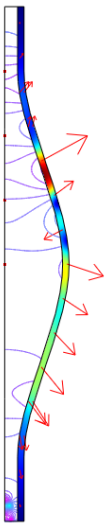

Figure 18: ***Geometry of the vicoelastic tube that represents an aneurysm, and which is deforming under the pressure pulse***: Arrows represent deformations of the wall, stream lines is the pressure inside the tube, and isosurfaces are the total displacement

The parameters, boundary conditions and entrance conditions are exactly the same than those of the simulation it the straight tube (See part 7.1).

The results of the wave propagation are plotted in Figure 19.
Regarding the previous simulation in the straight tube, we note that the arterial pressure in the aneurysm could be three times lower than in the regular one. We note that the pressure is not back to its typical value at the exit of the aneurysm.
Moreover, we observe a deacrease of the wave velocity - which was predictable, since the Moens Korteweg velocity is conversely proportional to the radius (See part 5.1, formulations (43) added with formulation of κ (35)).

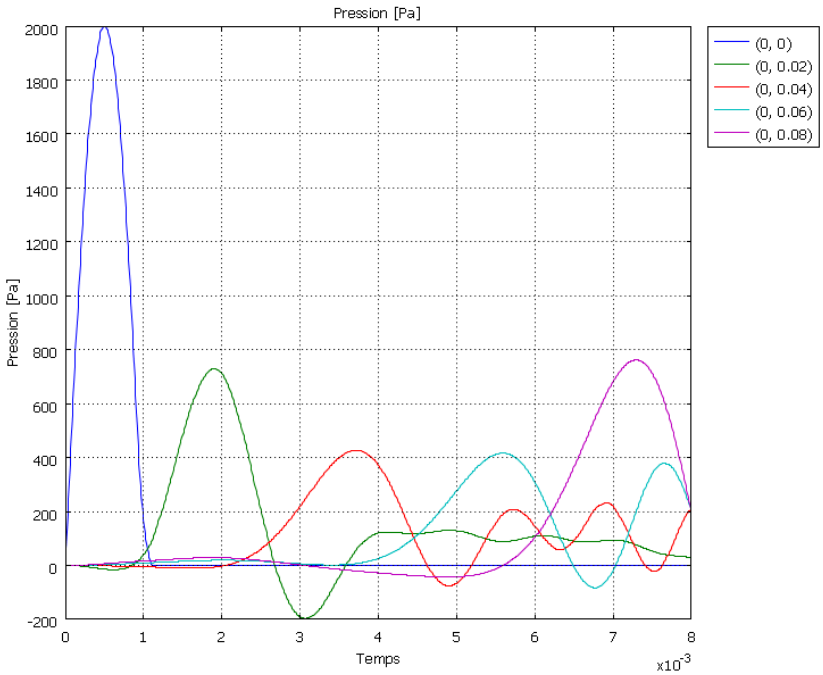

Figure 19: ***Propagation of a pressure pulse in a tube that represents an aneurysm***

A one-dimensional simulation is quite possible. But it is necessary to rewrite the model since the radius $R_o = R_o(x)$ is changing along the axis.
A difficulty in the formulation of the "new model" is the establishment of a characteristic wave velocity parameter. Indeed, it appears that the characteristic velocity C_o changes with the radius, and then, all the other parameters as well.
The analytical and numerical analysis needs to be done carefully to get a true wave propagation velocity all the axis long.

10 CONCLUDING DISCUSSION

The appearance of very small parameters in the vascular system encourage us to approximate the full 3D Navier-Stokes equations and use the *phenomenological analysis* to formulate simple one-dimensional model.

We have first considered a steady and pulsated flow in a rigid tube in order to formulate simple velocity profiles which depend on the value of the Womersley number (Part 2). These profiles have been used in the case of flows in flexible tubes, and have brought a "Womersley closure" that removed a unknown variable (Part 3).
Since then, the integral 1D equations have been formulated. It however miss a last closure that is formulated with the viscoelastic and non linear behaviours of the tube's wall (Part 4).
The establisment of the model without dimension allowed to define dimensionless parameters that will contribuate to the understanding of the wave propagation phenomenon (Part 5 and 6).
Finally, using the MacCormack numerical method, we have compared the numerical result of this one-dimensional model with, first a simulation made with the COMSOL 3.4 software, and then with experimental datas.

The results of the one-dimensional model, in comparison with the measurement datas and COMSOL 3.4, encourage to carry on use it for complex system.
However, it is necessary to find good theoretical agreement with the entrance parameters of experiments in order to carry out prediction works.

A interesting following study could be consider curved and bifurcating viscoelastic and non-linear tubes, and then quantify the effect of such geometry on the wave propagation.
Also, a challenge in the simulation of flows in vascular tubes is to consider non-negligible particles in the observed fluid.

ANNEXE 1* : *Demonstration of expressions for circumferential and radial stress component at the internal radius of a tube.

Let R_i and R_e be the internal and external radius, and p_i and p_e, be the internal and external loaded pressure. Humphrey D. gives us the expressions for circumferential and radial stress component through the thickness of the tube, where $R_i < R < R_e$:

$$\sigma_{\varphi\varphi}(R) = \frac{p_i R_i^2 - p_e R_e^2}{R_e^2 - R_i^2} + \frac{R_e^2 R_i^2}{R} \frac{p_i - p_e}{R_e^2 - R_i^2}, \tag{63}$$

$$\sigma_{rr}(R) = \frac{p_i R_i^2 - p_e R_e^2}{R_e^2 - R_i^2} - \frac{R_e^2 R_i^2}{R} \frac{p_i - p_e}{R_e^2 - R_i^2}. \tag{64}$$

As we are going to use the software COMSOL 3.4 in order to study the tube's deformation under the pressure load of a flow, we first take it in hand to verify these above formulation.

We use the structural mechanics application mode in a 2D and strain-plan formulation. The material is linear and elastic with a Young's Modulus $E = 2,0.10^{11}\ Pa$, and a Poisson's ratio $\vartheta = 0.33$. $R_i = 2\ m$ and $R_e = 5$. It is applied an internal pressure $p_i = 2,0.10^5\ Pa$, and the external pressure is set to zero.

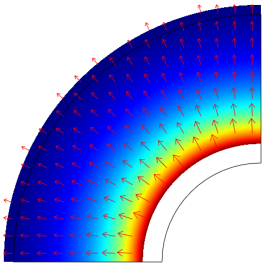

Geometry of a portion of a tube loaded with an internal pressure: Arrows represent deformations of the wall and isosurfaces are the first principal stress component

Thanks to the Hooke's Law written in the system [(28),(29),(30)], and using expressions of $\sigma_{rr}(R)$ and $\sigma_{\varphi\varphi}(R)$, we verify the used theory by ploting the both strain-displacement and stress circumferential and radial components:

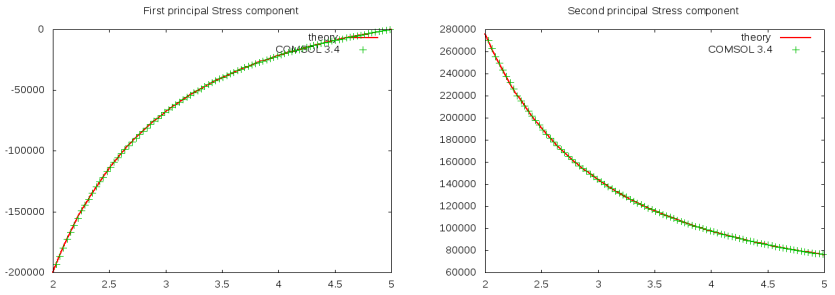

Stress components through the thickness of a portion of a tube: Comparison between theory and COMSOL 3.4. On the left is plotted the principal radial component depending on the radius lengh, and on the right is the circumferential depending on the radius lengh

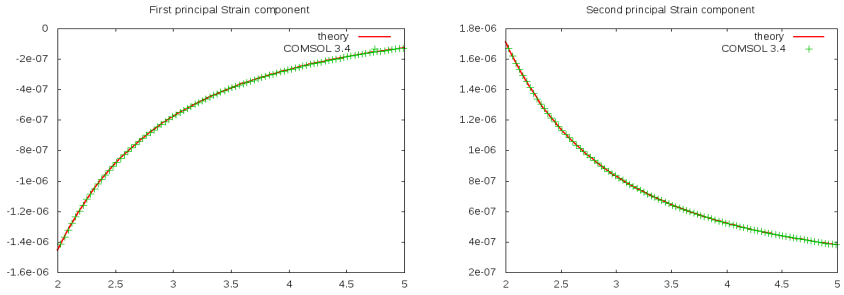

Strain-displacement components through the thickness of a portion of a tube: Comparison between theory and COMSOL 3.4. On the left is plotted the principal radial component depending on the radius lengh, and on the right is the circumferential depending on the radius lengh

Let us come back to our study. We are interesting in the deformation of the tube due to the pressure flow. In our case, $p_e = 0$ and $p_i = p(x,t)$ is the flow pressure.

$$\sigma_{\varphi\varphi} = \frac{pR_i^2}{R_e^2 - R_i^2}\left(1 + \frac{R_e^2}{R^2}\right), \tag{65}$$

$$\sigma_{rr} = \frac{pR_i^2}{R_e^2 - R_i^2}\left(1 - \frac{R_e^2}{R^2}\right). \tag{66}$$

With a tube of a thickness h, we have $R_e = R_i + h$. We are interesting in the deformation due to the pressure of the flow. So let us look after what is happening inside the tube:

$$\sigma_{\varphi\varphi}(R = R_i) = p\,\frac{(R_i + h)^2 + R_i^2}{h(2R_i + h)}, \tag{67}$$

$$\sigma_{rr}(R = R_i) = -p. \tag{68}$$

Here is the formulation used in section 4.1 .

***ANNEXE 2* : Detailed algorithm used in the numerical simulation.**

(We have forgotten the ' - ' reminding the dimensionless variables)

◇*Start time loop*
$r_i^n = 0$
$Q_i^n = 0$

◇*Inlet conditions*
$r_{i=0}^n = \dfrac{-\kappa + \sqrt{\kappa^2 + 4\lambda P_o sin(\pi t_n}}{2\lambda\varepsilon R_o}$
$Q_0^n = 2Q_1^n - Q_2^n$
$Q_{-1}^n = 2Q_0^n - Q_1^n$

◇*Outlet conditions*
$r_{n_x}^n = 2r_{n_x-1}^n - r_{n_x-2}^n$
$Q_{n_x}^n = 2Q_{n_x-1}^n - Q_{n_x-2}^n$

◇*Predictor step*
$r_i^* = r_i^n - \dfrac{\Delta t}{\Delta x}(Q_{i+1}^n - Q_i^n)$

If $\alpha \to 0$
$Q_i^* = Q_i^n - \varepsilon_1 \dfrac{4}{3}\dfrac{\Delta t}{\Delta x}\left(\dfrac{(Q_{i+1}^n)^2}{S_{i+1}^n} - \dfrac{(Q_i^n)^2}{S_i^n}\right) - \dfrac{\Delta t}{\Delta x}(r_{i+1}^n - r_i^n)$
$+\eta\varepsilon_{klv}\dfrac{\Delta t}{\Delta x^2}(Q_{i+1}^n - 2Q_i^n + Q_{i-1}^n) - \lambda\varepsilon_{nl}\dfrac{\Delta t}{\Delta x}((r_{i+1}^n)^2 - (r_i^n)^2) - \Delta t\dfrac{16\pi}{\alpha^2}\dfrac{Q_i^n}{(R_i^n)^2}$

If $\alpha \to \infty$
$Q_i^* = Q_i^n - \varepsilon_1 \dfrac{\Delta t}{\Delta x}\left(\dfrac{(Q_{i+1}^n)^2}{S_{i+1}^n} - \dfrac{(Q_i^n)^2}{S_i^n}\right) - \dfrac{\Delta t}{\Delta x}(r_{i+1}^n - r_i^n)$
$+\eta\varepsilon_{klv}\dfrac{\Delta t}{\Delta x^2}(Q_{i+1}^n - 2Q_i^n + Q_{i-1}^n) - \lambda\varepsilon_{nl}\dfrac{\Delta t}{\Delta x}((r_{i+1}^n)^2 - (r_i^n)^2) + \Delta t\dfrac{\pi\sqrt{8}}{\alpha}\dfrac{Q_i^n}{R_i^n}$

◇*Corrector step*
$r_i^{n+1} = \dfrac{1}{2}(r_i^* + r_i^n) - \dfrac{\Delta t}{2\,\Delta x}(Q_i^* - Q_{i-1}^*)$

If $\alpha \to 0$
$Q_i^{n+1} = \dfrac{1}{2}(Q_i^* + Q_i^n) - \varepsilon_1 \dfrac{4}{3}\dfrac{\Delta t}{2\Delta x}\left(\dfrac{(Q_i^*)^2}{S_i^*} - \dfrac{(Q_{i-1}^*)^2}{S_{i-1}^*}\right) - \dfrac{\Delta t}{2\Delta x}(r_i^* - r_{i-1}^*)$
$+\eta\varepsilon_{klv}\dfrac{\Delta t}{2\Delta x^2}(Q_{i+1}^* - 2Q_i^* + Q_{i-1}^*) - \lambda\varepsilon_{nl}\dfrac{\Delta t}{2\Delta x}((r_i^*)^2 - (r_{i-1}^*)^2) - \dfrac{\Delta t}{2}\dfrac{16\pi}{\alpha^2}\dfrac{Q_{i-1}^*}{(R_{i-1}^*)^2}$

If $\alpha \to \infty$
$Q_i^{n+1} = \dfrac{1}{2}(Q_i^* + Q_i^n) - \varepsilon_1 \dfrac{\Delta t}{2\Delta x}\left(\dfrac{(Q_i^*)^2}{S_i^*} - \dfrac{(Q_{i-1}^*)^2}{S_{i-1}^*}\right) - \dfrac{\Delta t}{2\Delta x}(r_i^* - r_{i-1}^*)$
$+\eta\varepsilon_{klv}\dfrac{\Delta t}{2\Delta x^2}(Q_{i+1}^* - 2Q_i^* + Q_{i-1}^*) - \lambda\varepsilon_{nl}\dfrac{\Delta t}{2\Delta x}((r_i^*)^2 - (r_{i-1}^*)^2) + \dfrac{\Delta t}{2}\dfrac{\pi\sqrt{8}}{\alpha}\dfrac{Q_{i-1}^*}{R_{i-1}^*}$

ANNEXE 3 :Using of COMSOL Multiphysics 3.4

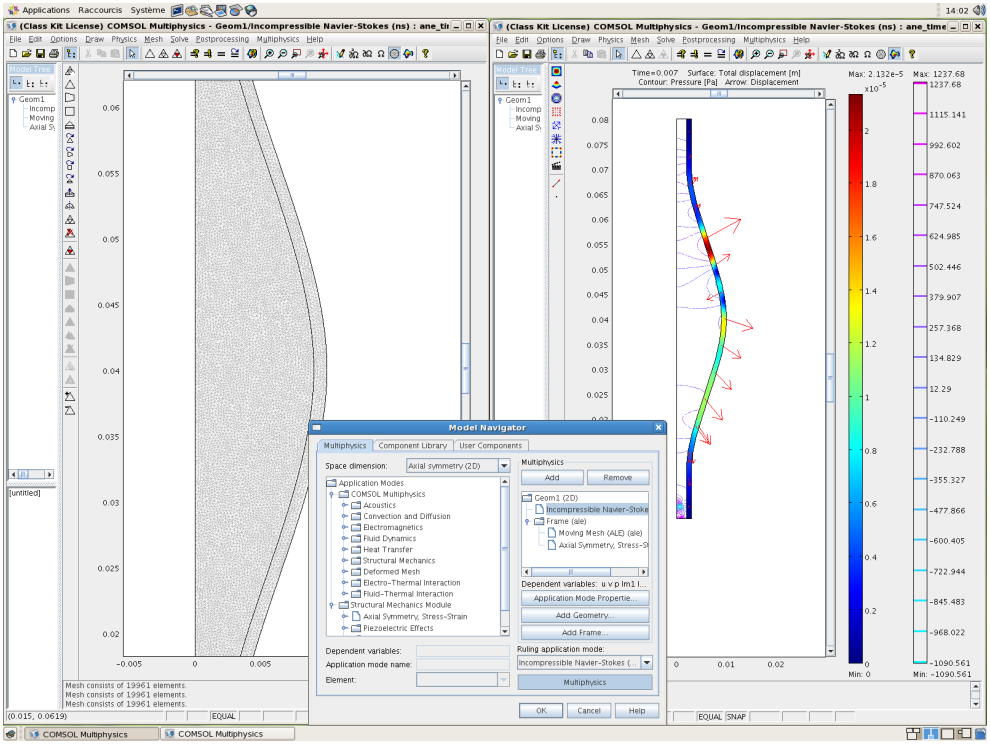

Screen Capture of COMSOL 3.4: On the left is reprented the used meshing for the simulation of the "viscoelastic aneurysm". On the right is the result of the simulation, and the under window represent the Model navigator.

REFERENCES:

[1] Comsol HELP: Chapiter 2 - Advance Modeling in COMSOL MULTIPHYSICS
[2] Fullana J.M., Zaleski S., *A branched one-dimensional model of vessel networks*, J. Fluid Mech. (2009), vol. 612, pp. 183-204, 2009 Cambridge University Press.
[3] Fullana J.M., *Gonflement tissulaire, élastopgraphie, et modèle d'oedème - Systèmes veineux et systèmes lymphatiques - Notes de cours*, Université de Pierre et Marie-Curie, (2009)
[4] Fung, *Biomechanics Circulation* (1997), Springer
[5] Horsten, Van Steenhoven, Van Dongen, *Linear propagation of pulsatile waves in viscoelastic tubes*
[6] Humprey Delange , *An Introduction to Biomechanics*, Springer
[7] Jaffrin, Goubel, *Biomecanique des fluides et des tissus* (1998), Masson.
[8] Lagrée P.-Y. (2000) *An inverse technique to deduce the elasticity of a large artery* , European Physical Journal, Applied Physics 9, pp. 153-163
[9] Monavon A., *Analyse Phénoménologique des écoulements - Notes de cours*, Université de Pierre et Marie-Curie, (2009)
[10] Pedley, *The Fluid Mechanics of Large Blood Vessels.* (1980), Cambridge University Press, Cambridge.
[11] Pindera, Ding, Athavale, Chen, *Accuracy of 1D microvascular flow models in the limit of low Reynolds numbers*, Microvascular Reaserch 77 (2009) 273-280
[12] Ritzenthaler, *Courbe de Bezier - Option agregation C* (2009)
[13] Stergiopulos, Young, Rogge, *Computer simulation of arterial flow with applications to arterial and aortic stenoses*,J. Biomechanics Vol 19, No 12, pp. 1477-1488, 1992.
[14] Tardy, Meister, Perret, Brunner, Arditi, *Non-invasive estimate of the mechanical properties of peripheral arteries from ultrasonic and photoplethysmographic measurements*, Clin. Phys. Physiol. Meas., 1991, Vol. 12, No. 1, 39-54.
[15] Van de Vosse and Van Dongen, *Cardiovascular Fluid Mechanics -lecture notes-* (1998), Eindhoven University of Technology, faculty of Mechanical Engineering (MaTe), faculty of Applied Physics (NT)
[16] Womersley, *Oscillatory Motion of a Viscous Liquid in a Thin-Walled Elastic Tube - I: The Linear Approximation for Long Waves* (1957), ...
[17] Zagzoule, Marc-Vergnes, *A global mathematical model of the cerebral circulation in man*, J. Biomechanics Vol 19, No 12, pp. 1015-1022, 1986

Internet Sources:

[1] $http://nptel.iitm.ac.in/courses/Webcourse-contents/IIT-KANPUR/FLUID-MECHANICS/lecture-31/31-1_entry_flow.htm$
[2] $http://www.zfm.ethz.ch/alumni/leutenegger/Numerical.htm$
[3] $http://ajpheart.physiology.org/cgi/content/full/293/4/H2355$
[4] $http://commons.wikimedia.org/wiki/File:Kelvin_Voigt_diagram.svg?uselang=fr$
[5] $http://en.wikipedia.org/wiki/Maxwell_material$